# Explorations in reaction times, and reaction times distributions, from chemical kinetics to visual memory

**Jacques Ninio**

Laboratoire de Physique Statistique
Ecole Normale Supérieure/PSL Research University
24 rue Lhomond, 75231 Paris cedex 05, France

e-mail: jacques.ninio@lps.ens.fr
Tel: (33) 1 44323318

Running title: Reaction times in molecular and mental processes

Keywords: chemical kinetics, molecular accuracy, visual memory search, reaction time patterns, alternating presentations

## Abstract

Recognition between molecules in molecular biology can be explained in terms of the structures of the interacting molecules, but also in terms of the relative durations of various steps in the representative reaction schemes. In this case, the calculations make use of the chemical kinetic formalism, according to which any reaction is represented by a concatenation of elementary steps, each step being an exponential decay. From there, one predicts an efficiency/accuracy tradeoff and may construct kinetic proofreading schemes. The knowledge of the reaction time (RT) distributions is essential to derive the correct results.

I review here my published work on RTs and RT distributions in "mental recognition" - more precisely, on the time to memorize an image and recognize it later. Past results are refined here by increasing the size of the data sets in order to obtain more precise RT histograms. Several clearcut results are presented, that deserve becoming central to an understanding of memory. They raise challenging issues for theoreticians, for instance why the time to memorize an image varies like the square of its number of elements, why recognizing symmetry between two images is faster than recognizing identity, how the brain decides, during a search in memory, that some hidden information is still there, or how the brain computes 3d interpretations from visual streams received at different times.

In an ambitious work on working memory retrieval, involving over 300,000 RT measurements, a striking dissociation between error rates and RT patterns was found. The RTs could be ordered on a map. This map, I conjectured, reflected the path for moving from slot to slot in a visual working memory store. RT patterns would thus reveal the organization of slots in a working memory store, in the same way that diffraction bands tell us something about the structure of a crystal.

Whenever possible, histograms showing the experimental RT distributions in visual memory tests are shown. They were modeled with a modification of the chemical kinetic formalism. Depending upon the complexity of the task, schemes with one, two or a few steps were adequate. The RT distributions derived from the kinetic schemes needed though to be complemented with a Gaussian widening, and a horizontal shift. This kinetic modeling will be illustrated with examples from visual patterns memory, symmetry perception, and shape recognition after inverting black and white.


## 1. Introduction: links between molecular biology and cognitive sciences

In molecular biology, it is said that an enzyme *recognizes* its legitimate substrate among competing analogs, that a ribosome *selects* a *cognate* transfer RNA molecule among the *non-cognate* or *near-cognate* analogous transfer RNAs, that an antibody *discriminates* between self and non-self antigens. The dominant explanations are based upon crystallographic data, from which rather static models of interactions are derived, involving "lock-and-key" complementarity between enzyme and substrate, or antibody and antigen (Fischer, 1894). Alternatively, one examines the detailed process through which, after an initial association with a substrate, an enzyme *decides*, so to speak,

whether or not it will transform it into product. In this case, structural descriptions are de-emphasized, and the kinetic details of the process are given a prominent role.

In cognitive sciences, there are a plethora of problems involving discrimination, recognition and decisions. I will expound and explore here some correspondences between the two bodies of knowledge. Actually, several inspirations taken from one field helped me progress in the other field.

We know from Köhlers' work that if a hen is trained to select food on a dark gray plate, and avoid a medium gray plate, then is tested on a pair of plates, a light gray and a medium gray one, it chooses the medium gray plate (Köhler, 1918)! In other words it selected the darker of the two plates. Its discrimination criterion was a relative one, not an absolute "lock-and-key" match with a particular shade of gray. There is no such relative choice in enzyme kinetics. Each encounter of an enzyme is with a single substrate, and results in a decision : "accept" or "reject". On the other hand, since the decision is the outcome of a probabilistic process, a correct substrate may be rejected, and an anlog may be accepted, as we shall see in Section 2. Moreover, there is room for a notion of competition inasmuch as the enzyme is confronted with substrate molecules that are outnumbered by analogs. This is the case of transfer RNA selection by ribosomes, and antigen presentation to T cell receptors in immunology.

Another connection between molecular biology (more precisely, the subfield of molecular accuracy) and cognitive sciences is in the status of *errors*. In molecular biology, people viewed errors as the outcome of aberrant processes, coexisting in the cell in parallel with the normal process (Gorini, 1971). In contradistinction, it has been very common in cognitive sciences, since Mach's profound analysis of the Mach band illusion (Mach, 1865) to view errors as resulting from the application of standard procedures. Errors (illusions) would thus reveal something about the mechanism of the standard processes. Errors also arise in a different way, and reflect uncertainty: This has practical importance in psychophysical experimentation. There is indeed an experimental tradition of setting up conditions in which a subject must choose between two stimuli, and the experimentalist makes the two stimuli more and more similar to each other so as to reach a stage of *just noticeable difference*. The just noticeable difference criterion is usually coupled with an *alternative forced choice procedure* (AFC). The subject is forced to choose one stimulus or the other, he/she is not allowed to (admit) his/her ignorance. When the just noticeable difference stage is reached, the subject answers almost at random, he/she makes nearly 50% errors. Incidentally, this method may generate illusions, especially in the tactile domain. If you are tested on your sensitivity to pricks under conditions of frequent stimulations, you may occasionally feel that you are being pricked, but nothing happened. This is the theme of 'false positive' responses.

My main contribution to molecular accuracy was inspired by Köhler's problem on training in hen – is recognition absolute or relative? Later, I applied to one field ways of thinking borrowed from the other. One anecdotical example is in a work on geometrical visual illusions. I needed to explain a result by the Swiss evolutionist and cognitivist Jean Piaget (see Piaget, 1974 for the two facets of his talent), and I found that a property of convex functions might underlie his results (Ninio, 1979). This property was just what I needed to prove a result in the kinetic theory of accuracy (Ninio, 1977) so there was a same explanatory figure in the two articles.

In addition to the common set of problems of choice and decision, the main bridge between the two domains, in my case, was a technical one, in the attention given to timing

aspects. This article is mainly a review of my contributions in which conclusions were drawn from reaction times and reaction times distributions, either in molecular biology, or in visual perception and memory. In the first case the work was theoretical, and in the second case, I produced the data myself.

## 2. Recognition and reaction time distributions in molecular biology

A key concept in molecular biology is that of "specificity". There are thousands or even tens of thousands of different species of molecular components within a cell, all of them moving more or less randomly within the confined cellular volume, bouncing against each other, sometimes sticking together for a certain amount of time, then falling apart or undergoing a chemical transformation through their interaction. Yet, the cell behaves in an extremely precise way. During the replication of DNA, its genetic material, there are merely six errors per $10^{10}$ replication steps in a bacterium (Drake et al., 1998; Elez et al., 2010), or one error per $10^{8}$ replication steps in man (e.g., Kong et al., 2012). In the most frequent situation, there is a molecular encounter between two partners: an enzyme – a large molecule that will perform a catalytic act, and a substrate that the enzyme will transform into a different product. Enzyme specificity must be rather high. This means that when an enzyme encounters a chemical compound upon which it is supposed to act (its "substrate"), they stick together, and the catalytic act succeeds with a reasonably high probability, but when the enzyme encounters a related chemical compound (an "analog"), either they do not stick at all, or they stick, and the catalytic act aborts with a high probability.

This probabilistic description does not follow the dominating "lock-and-key" concept. According to this concept, an enzyme binds to its natural substrate, when they fit like a lock with its key, in which case the catalytic act is performed with a near to one probability. The enzyme does not bind to the analogs, and there is no chance that the enzyme will modify the analog; the enzyme-substrate interactions would be essentially error-free. The lock-and-key concept was introduced in the 1890's (Fischer, 1894) to explain immunological specificity. It was thought that the specificity of the immune system relied upon exclusive interactions between invading molecules (the "antigens") and defender molecules (the "antibodies") produced by B cells. The antibodies that were manufactured to get rid of the invaders were thought to be extremely specific. This turned out to be false and instead there is a growing body of data on antibody multispecificity. Here also we can speak of a cognitive act, and of the problem of how to make a correct decision when there are so many cross-interactions between antibodies and antigens. A good deal of the problem is in distinguishing external invaders from internally produced compounds that can be targets to the antibodies, thus generating autoimmune diseases. This is also debated as the "self" versus "nonself" discrimination issue. Part of the solution came when it was realized that another class of cells of the immune system — the T cells — played a crucial role in the decision process. Now, the antibodies could be viewed as not too specific weapons, and the decision to shoot at a target was under the control of a different class of molecules — the T cell receptors. There was however a serious problem on how to couple the decision (to shoot or not to shoot) with the most adapted cellular weapon producers. Part of the solution came when the role of still another class of cells of the immune system — the dendritic cells — started to be clarified, but this will take us too far. I just point out here that there is another theoretical problem with

dendritic cells. Since they work, in part, as nonspecific antigen collectors, there is the question of whether or not they can segregate different antigen species in separate clusters at their surface (Ninio and Amigorena, 2004). I have insisted on immunological specificity, because it may provide rich metaphors for cognitive problems.

I now deal with enzyme specificity, a field that will allow me to develop practical connections with the reaction time distributions in my visual memory experiments. A series of observations on enzyme specificity, in the 1970's, required serious amendments to the classical lock-and-key explanations. These were made in both the fields of protein synthesis with which I deal here, and DNA replication.

In protein synthesis, an extremely complex molecular machine, the ribosome, reads a sequence of instructions on a messenger RNA and performs the synthesis of a protein according to the sequence of small units A, U, C, G on the messenger RNA. This process is less accurate than DNA replication (about one error per ten thousand amino acid incorporated into the nascent protein). By mutations, ribosomes were generated, that were either more error-prone or more accurate than the standard ones. It is not surprising that a very simple mutation may make the ribosomal machinery less accurate. On the other hand, the fact that this machinery that had been optimized during about three billion years of molecular evolution could be readily improved by simple mutations was baffling. It would seem that evolution did find the way to boost accuracy beyond its present level, but settled to the present level for energetic or other optimization reasons, while maintaining an “accuracy reserve” within reach. An analogy coming to mind is that of human memory. It is a major evolutionary achievement, you would not anticipate that some minor genetic modification might boost memory by an enormous factor, yet people with exceptional memories do exist (e.g., Wilding and Valentine, 1997), and this does not even seem to be attributable to a mutation. Attempts to explain the origin of the hyper-accuracy of the hyper-accurate mutated ribosomes (Gorini, 1971) were ad hoc and unsatisfactory, until it was realized that there could be an underlying efficiency/accuracy tradeoff (Ninio, 1974).

More precisely, I introduced the notion that once a ribosome and a substrate made their encounter, they would stick together for a certain amount of time *theta*, during which the ribosome had a chance to accomplish its catalytic act. The *theta*’s would be large for the correct substrates, and small for their undesirable analogs. The catalytic act was postulated to occur with a certain probability per unit time, so there would be a characteristic decision time *tau*. The analysis showed that in a general way, accuracy was governed by the ratio between the *theta*’s (how much time is given to make a decision) to the *tau*’s (how fast one takes a decision within the available time). In the limiting case in which the responses are very fast with respect to the stimuli durations (the *tau*’s are small with respect to the *theta*’s) there will be a response with a close to one probability, whether the substrate is the cognate one or not ; accuracy is then rather low. At the other extreme, when the responses are very slow (large decision times *tau*’s compared to the *theta*’s), many encounters between the protein synthesis apparatus and a substrate will be unproductive. The partners will fall apart unproductively. There will be a small proportion of successful catalytic acts, and the probability of success will increase as the sticking times increase, so accuracy will be higher, but at the cost of having an important proportion of abortive interactions. So, it is a case of efficiency/accuracy tradeoff. The overall speed of the process is mostly a side-effect of the abortion rate.

The mathematics were rather simple to work out, they relied on the classical understanding of reaction rates in enzyme kinetics. A reaction scheme is described by a

more or less complex “wiring diagram” (see for instance Fig. 1). It is postulated that the enzyme may be in a number of different states : free in solution, or bound to a substrate, or bound to the product of the catalytic act, prior to the departure of the product. Furthermore, there may be several different states of the free enzyme, and several intermediate states along the reaction pathways. The schemes indicate the possible transitions between states. Kinetic constants (the k’s in Fig. 1) are assigned to each transition, and they have a precise implication according to chemical kinetic theory : every transition is assumed to occur with a constant probability per unit time (like radioactive decay). It is independent of the past, history does not count. The scheme may include reversibilities — there would be transitions from a state A to a state B, and from the state B to the state A, it may include branchings, or even loops. With just a few sates, a very rich phenomenology can be generated, and it has been worked out in enzymology, under the names of allostery, kinetic cooperativity, half of the sites reactivity, etc.(e.g., Cornish-Bowden, 2012). Explicit expressions for average reaction rates are often easy to derive. For a long time, enzymological discussions of reaction rates were made in terms of large population of enzymes, so reaction rates were considered to be averages over large populations. However, these instantaneous averages on enzyme populations are the same as the averages for a single enzyme molecule that would be followed during a very large number of cycles of substrate binding and product release (in practice, see Ninio, 1987).

---

Insert Figure 1 about here

---

Given a reaction scheme, and the kinetic constants for the cognate enzyme-substrate interactions, and the non-cognate interactions as well, it is easy to compute the error-rate. Mathematically, this is straightforward, yet there is a conceptual subtlety : reaction time distributions are essential to understand the results. This is due to the fact that all kinetic constants are characteristic parameters of probabilistic processes that extend from time zero to infinity. A sticking time $theta = 1/k_{-1}$ corresponds to a situation in which the enzyme and the substrate have a probability of falling apart = $k_{-1}$ dt per elementary time dt. A processing characteristic time $tau = 1/k_2$ corresponds to a situation in which the enzyme has a probability of success of performing the catalytic act = $k_2$ dt per elementary time dt. Therefore, a situation described by two kinetic parameters *theta* and *tau* includes events in which a sticking time is rather large and a processing time very short, and inversely events in which dissociation is rapid and occurs before processing has a chance to occur. Taking into account the probabilistic distributions of the *theta*'s and the *tau*'s one gets, for most simple reaction schemes (the Michaelis scheme (c) in Fig. 1) a remarkably simple formula: the probability of a productive interaction is p = *theta*/(*theta* + *tau*). Then the error-rate follows an *efficiency/accuracy* tradeoff. A *speed/accuracy* tradeoff is often observed and discussed in psychophysical experiments, and a wealth of models were devised to account for the experimental observations (for instance, Wickelgren, 1977; Luce, 1986; Bogacz et al., 2009).

Ways to construct reaction schemes to boost accuracy beyond what was anticipated from standard kinetic schemes were proposed, under the names of “kinetic

proofreading“ or “kinetic amplification“ (Hopfield, 1974, 1980 ; Ninio, 1975, 2006). The essential trick is to introduce a time-delay before initiating the processing stage. Imagine for instance a substrate with a sticking time *theta* = 100 ms, and an analog with a smaller sticking time *theta* = 10 ms. If the enzyme is prevented from accomplishing the catalytic act during the first 20 ms after binding, then the probability of accomplishing the catalytic act is slightly diminished for the correct substrate, and very substantially reduced for the analog. The main difficulty was to construct a scheme that would involve a (probabilistic) time-delay, and satisfy the thermodynamic constraints of chemical kinetic theory. The kinetic proofreading ideas are well accepted in the protein synthesis field, and they have been adapted to several other fields, including immunology (McKeithan, 1995). They should not be confused with more classical ideas on accuracy, such as the use of redundancy for reliable computation (e.g., Winograd and Cowan, 1963).

There is a different, dominating tradition in mathematical enzymology, in which rates rather than times are considered, and one analyzes the fluxes between states in large populations of molecules, instead of transition probabilities. In cognitive sciences, one is more inclined to discuss decision times, but some authors are attempting to introduce rate distributions as an alternative to time distributions (e.g., Harris et al., 2014).

## 3. Time to compare two images side by side

This work was inspired from a well-known visual game in which two drawings of a complex scene differ at seven positions, and the task is to locate the differences, which can take a surprisingly long time. In searching for the differences the eyes try to capture part of one image, then move to the corresponding part of the other image, and although the two images may differ in this region, the person may not detect the difference. The explanation is that when the person looks at the first image, he/she extracts partial information, which is held in short-term visual memory (STVM) while he/she performs a visual saccade to the other image. Upon visual landing on the appropriate portion of the second image, the person compares the available detailed visual input from the second image with the representation of the first image in STVM. Failure to detect the difference is an indication that the STVM representation was not detailed enough to include pertinent information about the locus of the difference between the two images.

---

Insert Figure 2 about here

---

Nicolas Brunel and I attempted to determine the capacity limit of STVM by measuring the time to locate a difference between two artificial images presented side by side on a computer monitor as a function of their complexity. Our hope was to detect a sudden rise of reaction times above a certain level of image complexities. The images were abstract patterns — square lattices filled at random with black or white quadrangles (examples in Fig. 2, top row). Two images were presented side by side, and the right image differed mainly from the left one by a white/black inversion in one of the

quadrangles. The task of the subject was to compare the two images, until he/she spotted the difference between the two images.

For images of size NxN, the median reaction time for locating the difference varied as $cN^2$, from N = 3 to N = 15, with c being around 50 ms in the absence of grid. (i.e., when the quadrangles were associated into continuous shapes). The relationship was clearcut but disappointing – there was no discontinuity that might have suggested the existence of capacity limit in STVM. Errors and RTs followed similar courses over the range of experimental conditions. There were though some interesting side results — see the legend to Fig. 2. The results taken together indicate that the detection of differences does not proceed on a pixel by pixel representation, and must be mediated by an abstract shape analysis.

---

Insert Figure 3 about here

---

Brunel and I then implemented another protocol. The images to be compared were similar in 50% of the cases, and differed at a single position in 50% of the cases. The subjects had to judge whether two images presented side by side were the same or different, with N varying from 1 to 5 (Fig. 2, bottom rows). When images are different, and the subject moves his/her eyes from one image to the other, the search terminates as soon as the difference is located. When the images are the same, the similarity may be obvious at a low level of image complexity, but at a higher level of complexity, the subject must move his/her eyes from one image to the other and in this case he may need to make a complete back and forth exploration to be sure that there is no difference between the two images. For $N \leq 3$, the same and the different responses were similar in all their statistical aspects. For $N \geq 4$, the "same" responses took a significantly larger time than the "different" responses and were accompanied by a significant increase in false negative errors — a subject may judge two different 4x4 images as being identical. This is a form of "change blindness", as pointed out by Scott-Brown et al., 2000. The qualitative change from N = 3 to N = 4 is interpreted as a shift from a "single acquisition" analysis to a scanning procedure. On the whole, we suggested that visual information in our simultaneous comparison task is extracted by chunks of about $12 \pm 3$ bits (counting one black or white quadrangle as a bit), and that the visual processing and matching tasks take about 50 ms per couple of quadrangles (Brunel and Ninio, 1997). Data for comparisons of blocks of colored patterns, or blocks of letters are presented in Ninio, 2011. Here, I complete the 1997 Brunel and Ninio experiments on several subjects by testing myself on 2x2, 4x4, 6x6 and 8x8 pairs of same or different images. The RTs are shown in Fig. 3.

In Fig. 4, I show the RT distributions for 2x2, 4x4 and 6x6 images separately for the "same" and the "different" pairs of images. All RT distributions have the shape that is classically found in psychophysical experiments: there is a dissymmetrical bell-shaped curve that rises steeply after a lag, then declines slowly. This lag must reflect, in part, the time elapsed between the decision reached by the brain and the recording of the motor response, – a key press on the mouse of the computer. But it must also reflect other

contributions, since the RTs for motor responses were found, in several studies, to be often < 0.3 s. As the complexity of the images increase, from 2x2 to 6x6, the distributions become wider and wider. The increase in variance is easily justified, because the number of possible stimuli increases from 16 “same” and 64 “different” pairs of images in the 2x2 case, to $2^{36}$ “same” and $36x2^{36}$ “different” pairs of images in the the 6x6 case. In order to simulate these RT distributions, I use a model that was introduced previously in an earlier work on symmetry perception (Ninio, 2011). It is explained again in the Appendix.

---

Insert Figure 4 about here

---

The model involves three components : First, a “kinetic core”, as simple as possible, taken from the almost infinite possibilities offered by the chemical kinetic formalism, for example, any of the schemes shown in Fig. 1. Next, the RTs computed from the kinetic core are shifted by a lag, typically around 0.8 s. Last, the RT distributions are convoluted with a Gaussian of variance *sigma* square – *sigma* being expressed in seconds – that takes care of the many sources of variability not included in the kinetic model. Typically, the *sigma*'s were in the 0.05 s to the 0.1 s range.

As I show in Fig. 4, the kinetic core reduces to a single step (scheme (a) in Fig. 1) for both 2x2 similar and different images. It reduces to a Michaelis scheme (scheme (c) in Fig. 1) for both 4x4 similar and different images. It can be seen that the RT distribution is wider when the images are similar, which is logical. This flattening of the distribution is accounted for by a decrease of all 3 kinetic constants of the kinetic model. With 6x6 images, the kinetic core grows in complexity. We can model the RT distributions for the different images with a linear scheme involving two reversible steps, followed by a terminal irreversible step (scheme (d) in Fig. 1). A still more complex kinetic core was needed to account for the RT distribution for 6x6 same images – model (f) with three reversible steps and a branchpoint. For more details, see the legend to Fig. 4. The increasing complexity of the models is justified, taking into account the increased complexity of the task : construct a representation of the images, capture a part of one image, move the eyes to the corresponding location in the other image, move the eyes to another position in this image, move the eyes to the other image, and so on.

For a given class size (for instance 6x6), the stimuli can present widely different difficulties in the comparison tasks. This contributes to the breadth of the RT distributions. We do not have yet theoretical models of the factors that make pairs of images more or less easy to compare, although we can discern a number of criteria. In particular, an image can be decomposed into a number of all-black or all-white blocks. The simplicity of this decomposition plays a role in constructing a representation of the image, and the preservation or non-preservation of this decomposition in a pair of images, is an important factor in the detection of their difference, when there is one.

In most psychophysical studies, the stimuli are rather less complex than those used here, and the 'same' responses are usually faster than the 'different' responses (see van

Zandt et al., 2000). Here there is a hint for this trend at the smallest complexities (see the results in Fig. 3). The most gratifying aspect of our results here is the agreement between the complexity of the tasks, and the complexity of the kinetic schemes required to model the results.

## 4. RT distributions in symmetry perception

There is an abundant literature on symmetry detection – mainly vertical symmetry detection (e.g., Tyler, 1996). When two identical images are presented side by side, it may take you some time to realize that they are identical. However, if one of the images is juxtaposed, along one of its vertical sides, to its symmetrical image, the symmetry jumps to the eyes. The fact that vertical symmetry is far more salient than identity is rather well established (Bruce and Morgan, 1975).

---

Insert Figure 5 about here

---

I extended my previous work on comparing images side by side to pairs of images that were related by a vertical symmetry axis, and in which one of the elementary squares could be different (see examples in Fig. 5). So, at a rough level of description, the pairs were always symmetric, and the question became how good we are at detecting a small dissymmetry between the patterns – a symmetry violation. In the field of symmetry perception, the side by side presentation of similar images is called “repetition”. In this respect the work described in the previous section was about the detection of repetition violations. I performed, as a subject, extensive experiments on repetition violations and symmetry violations and in this case, both with separate and non separate images. Some reaction time distributions from Ninio, 2011, are shown here in Fig. 6.

---

Insert Figure 6 about here

---

The reaction time distributions are much narrower in the case of the symmetry condition. The distribution for 3x3 patterns can be modelled, in the case of symmetry with a model involving a single step (Fig. 1a), and in the 4x4 and 5x5 symmetry condition, with a two-step model (Fig. 1b). A two step model was also sufficient to account for the 4x4 repetition case and, to a rough approximation, for the 5x5 repetition cases (Ninio, 2011). However, the 5x5 RT distribution for repetitions appears to be bimodal, and a finer

analysis is now proposed in this review by separating the "same" from the "different" responses, see Fig. 4. The kinetic models for the nine histograms were remarkably consistent – see Table 1 in Ninio, 2011. All lags were between 0.8 and 1.0 second; all Gaussian *sigma*'s were between 0.04 and 0.07 second. They increased with the complexity of the stimuli. The kinetic constants $k_2$ for the 3x3 repetition, and the 4x4 and 5x5 symmetry conditions were around 20/s. This "fast" constant probably reflects the terminal (decision) step in the process. It falls to 5/s and 3/s in the 4x4 and 5x5 repetition experiments. However, in the refined, more complex models of Fig. 4 in the preceding section, all the terminal (decision) kinetic constants are in the 10/s to 15/s range. In the case of 3x3 symmetry violations, the model involves a single step, and $k_2$ fuses with $k_1$. Otherwise, the $k_1$'s decrease regularly with the complexity of the stimuli, from 8/s to 2/s in the symmetry experiments, and from 19/s to 3/s in the repetition experiments. The $k_1$'s probably reflect, in large measure, the time to construct a representation of the stimuli to be compared.

A most striking aspect of this kinetic modelling is the *absence* of a feature that might have been present: There is absolutely no room for an additional "mental flipping" step in the symmetry data. If such a step existed, it could have been reflected in an increased lag, an increased Gaussian widening, or the need for an additional kinetic constant $k_3$. Quite to the contrary, none of the 4 parameters gives an advantage to repetition comparisons. This raises the possibility that the representations of a pair of mirror-images are constructed faster than the representation of a pair of same images.

A possible explanation is that there is a potential artefact in the repetition experiments. A shape is, so to speak, contaminated by the neighbouring shapes. The perception of the left column in the right image is influenced by the patterns (and especially the black/white balance) of the neighbouring right column of the left image. Using another terminology, I would say that the perceptual groupings in one image are influenced by the features that are present on the closest border of the other image. Therefore, when two identical images are presented in the repetition mode, several groupings may be tried. They would compete, as in a Stroop effect, thus lengthening the reaction times. In contradistinction, the equivalence between the two sides of the symmetry axis in the symmetric presentations could force the spread of the same perceptual groupings in the two images of a symmetric pair. This conjecture might be tested in the future by exploring situations in which complementary information are sent simultaneously (Nimi et al., 2005) or asynchronously (van der Vloed et al., 2005) to the two eyes, and studying the reaction time distributions as a function of the presentation delays.

However, there may be a more profound cause for the superiority of symmetry over repetition judgements. Humans' general difficulty in distinguishing a shape from its mirror image led to the proposal (see, e.g. Corballis and Beale, 1971) that when the brain represents a shape, it constructs automatically the mirror-image representation of that shape. This is what I call a "folded sheet" model because it is reminding of Rorschach method for producing symmetrical shapes from inkblots squeezed between the two halves of a folded sheet. In a remarkable case study, Pflugshaupt et al. (2007) described a patient who, after a cerebral damage produced by hypoxia could not read normal text or write in the standard way, but could read text reflected in a mirror, and write in mirror-inverted way. The authors interpreted their data in terms of a folded sheet model: the brain, under normal conditions would construct both the normal representation of a visual stimulus, and its mirror-inverted form. Following a brain damage in some specific site, the standard

representation would be unavailable, and the brain would use the mirror-image representation.

I thought of an alternative possibility. I conjectured that somewhere in the brain, patterns would be represented like images printed on a transparent sheet: depending on the side of the sheet you are looking at, you see this pattern in its standard form, or in its mirror-inverted form (Ninio, 2011). Assume that two bundles of neurons have access to this representation from two sides, one bundle connecting the representation, say, to the left hemisphere, and the other connecting it to the right hemisphere. Then, through learning, a child would acquire a mechanism that inhibits the functioning of one of the two bundles, at least during reading and writing. If, due to brain damage, the main bundle cannot operate, inhibition can be removed, and the person would become able to read and write in mirror-inverted way.

## 5. Acquisition of information in visual memory, as a function of presentation time and number of images to recall

### 5.1 The time course of information acquisition

Having determined the amount of visual information that is extracted in a single shot and maintained in short term memory, I then explored the properties of visual information storage in a longer time range. I first studied visual memory of single images. An image similar in design to the images that were used in the previous section (slightly distorted square lattices of black or white quadrangles) was memorized for a certain amount of time, then it disappeared from the screen. Then a pair of images were presented side by side. One of the images was the memorized image, and the other one differed from this one at one or more positions, in which the quadrangles' colors were changed from black to white, or vice-versa. The task was to determine which of the two images corresponded to the memorized image. The amount of memorized information, expressed in bits, was deduced from the error-rate, as explained in Ninio, 1998.

I tested myself to determine how much I memorized of an image as a function of the presentation time, and the result was clearcut. The number $n$ of memorized bits varied roughly as the square root of the presentation time. (More precisely, the exponent x of the power law $n = t^x$ could be 0.56 rather than 0.5). The power law applied from a few seconds presentation time to at least 100 seconds (Fig. 7, right panel). To turn it differently, in order to double the number of memorized bits, I needed a presentation duration multiplied by four. Such a power law had in fact been described a century ago by Binet, 1894, in his observations on mnemonists who memorized large lists of numbers (Fig. 7, left panel). I also determined the amount of memorized bits as a function of presentation time when 2, 3 or 4 images were memorized consecutively, the images being tested in their presentation order. The number of memorized bits per image was smaller than in the case of single images, but the power law applied, with the same exponent. So, I confirmed with myself (a non-exceptional subject) and in the visual domain what had been observed with mnemonists in the 19th century. This power law should stand as one of the basic experimental laws of memory. Yet, it is largely ignored by memory specialists (but see Wilding and Valentine, 1997).

---

Insert Figure 7 about here

---

I then ran a series of experiments to determine what happened in a shorter time range, actually from 1 second to 8 seconds. This time, 30 naive subjects took part in the experiments. I determined the average number of bits memorized per image, for presentation times of 1, 2, 3, 5 and 8 seconds. I obtained a sigmoid dependency (Fig. 8). For one second presentations, about 12 bits were memorized - just the amount that had been found for short term visual memory and, presumably, acquisition times in the range of 300 ms. So, one could say that there is an initial capture of about 12 bits of information in about 300 ms, and no clear gain up to one second. Then, at 2 s presentation time, there is a small gain. The number of memorized bits rises to about 15. I interpret this increment as follows: With a 2 s presentation time, the subject can make a rapid exploration of the image, and choose a part which looks simple to memorize, on which he may fix his/her attention. So the gain would have little to do with the workings of memory. From 2 to 6 seconds, the curve is nearly horizontal, there is very little gain, but after six seconds, the curve starts ascending clearly. The stability in performance of the naive subjects between 2 and 6 seconds memorization is amazing. Furthermore, it contradicts the subjective feeling of acquiring information all along the presentation duration. In my opinion, what happens is that there is a first acquisition of visual information at the 12-15 bits level, up to two seconds presentation time. Beyond this first seizure of information, during which a few salient shapes within the image (for instance, a cross, a square, the letter T) were perhaps noticed, one needs to establish a dialog with long term memory to be able to construct a more detailed representation of the image. This is where an experienced subject can do better, because he/she has a larger store of readily accessible patterns in memory, that can match the patterns in the image, and a large store of criteria (are there alignments ? is there symmetry ? do the elementary patterns touch a border of the image ? and so on). A similar time-course was observed in parallel experiments in which two images had to be memorized, instead of one. In any event, the results are there (Fig. 8) and, to my knowledge, they are absolutely original in the field of memory.

---

Insert Figure 8 about here

---

## 5.2 How the retrievable information varies with the number of items

Having cleared the ground, I then proceeded to the more ambitious task of determining how the amount of memorized information varied with the number of memorized images. Would we, at last, find some evidence in favor of the mythical “magical number” ? I performed comparative experiments with several subjects attending to 1, 2, 3, 6, 12 images, up to 100 images.

I found, with three subjects, that when viewing *m* consecutive images, the average amount of information captured per image varies with *m* in a stepwise fashion. The first two step boundaries were around *m* = 3 and *m* = 9-12 (Ninio, 1998). Thus, instead of the expected magical number limit of 5-9 items beyond which nothing could be retained, we had a continuous stepwise curve. The data were interpreted, at that time, with a model of organization of working memory in successive layers containing increasing numbers of units, the more remote a unit, the lower the rate at which it may acquire encoded information. In later experiments with two additional subjects, I found a first boundary in the 4-6 range.

The differences between the subjects could be rationalized in terms of a filling strategy : subjects differed by their way of placing the images in different layers of a memory store. One subject would place them at random, another one would place the first images in the closest layers, in which storage accuracy was high, and another one would place the first images in the remote layers, where storage accuracy was low, then fill the memory store from the back. In this case, there is the paradoxical possibility that 9 images may be better memorized, on average, than 4 images, because the 4 images would be memorized at the lowest accuracy level !

I then tried to obtain detailed information on the quality of memorization of each of the images memorized within a set of 4 images in block-trial experiments.

There were incomprehensible discrepancies between error-rates and reaction times. Furthermore, when the testing order was reversed (from 1, 2, 3, 4 to 4, 3, 2, 1) the error-rates and the RT's for each image in a set of 4 could not be anticipated from the error-rates and RT's in the standard order. Furthermore, I did test myself systematically, using various testing order (e.g., 3-1-4-2, 2-3-4-1, etc). The results seemed erratic. It was not possible to characterize a "memorization quality" for each of the 4 images memorized in succession. It was not possible to predict the results obtained with one testing order from the results obtained with other testing orders. There were also discrepancies between the error-rates and the RT variations. Conceivably, when the experiments made use of a particular testing order, memory was adapting to this order and somewhat optimizing the placement and retrieval strategy of the items to this order. So I decided to run experiments in which the testing orders were randomized.

## 6. Visual memory experiments with random testing orders

If a subject views N images numbered 1, 2, …., according to their presentation order, there are 2 possible testing orders for two images, 6 possible testing orders for 3 images, 24 testing orders for 4 images, N! possible testing orders for N images (see the protocol in Fig. 9). Memory experiments were performed with a few subjects on blocks of N = 2 to N = 5 images, with random testing orders. Over 300,000 RTs were collected (Ninio, 2004). I focus here on the results for N = 3, because they display all the essential elements found in the other series.

---

Insert Figure 9 about here

---

Recognition errors are a function of the presentation order and the testing order. However, the 9 expected error-levels reduce to 4 (Fig. 10, left panel). One is applicable to images 1 and 2 at all testing orders, the other is applicable to image 3 – the last memorized image in a block of 3. It is very low when image 3 is tested first. The privilege of the last viewed, first tested image, over all other images, is extremely strong, in agreement with Phillips' picture of STVM (Phillips, 1974). On the other hand, the persistence of this privilege beyond the first testing stage was quite unexpected. Should we not expect each couple of images used in the tests, to occupy STVM one after the other? If this happened, the last memorized image should have lost its privilege immediately after the first test.

The results on reaction times contained even more exciting structural details which were not present in the error-rates results (Fig. 10, right panel). The RT for responding to a test on a given image at testing stage 2 or 3 depended significantly on which image was tested just before. For instance, the RT for a test on image 3 at testing stage 2 was shorter when image 2 was tested at stage 1 than when image 1 was tested at stage 1. The difference in RTs was observed despite the equality in error-rates for the two conditions. So, it is as though image 3 was maintained at a certain quality level at stage 2, but was more accessible to a memory search after a test on image 2 than after a test on image 1.

---

Insert Figure 10 about here

---

You can think of many models to account for such an observation. For instance, imagine that images 1, 2 and 3 are like aligned cars in a parking space. If you walk from one car to the other, it may be easier to reach car 3 from the location of car 2, than from the location of car 1. This is just one crude model to account for a single observation. However, the 6 testing permutations generate 12 different RTs on successive tests (6 for each stage 1- stage 2 succession, 6 for each stage 2 – stage 3 succession). The set of the 12 RTs was not as simply structured as the example chosen above suggests. Actually, the dominant pattern can be conceptualized by putting two images on one line, and the third image on another line, thus :

---- 1 --------- 2 ----

---------- 3 ---------

Imagine that downward motion is easier than upward motion, and that lateral motion is even more difficult than upward motion. Then you would have fast transitions from 2 to 3

or from 1 to 3, slow transitions from 1 to 2 and from 2 to 1, and intermediate transition times from 3 to 1 and from 3 to 2 .

From the set of inequalities between RTs on successive tests in both the 3 and the 4 images results, I derived a hypothetical geometrical model for a short term visual memory store (Ninio, 2004, and here, Fig. 11).

---

Insert Figure 11 about here

---

There are four rows of slots in the model of Fig. 11. The storage accuracy is assumed to decrease from row 1 which contains STVM to row 4. At the end of the active memorization phase, the last image is in the first row, and all previous images occupy the fourth row, if space permits. Metaphorically, you may imagine a parking space with one entrance. When cars are coming in, you accommodate them by lining them at the back. Late comers are parked closer to the entrance. As testings proceed, the last image moves up along the midline A-C-F. This description accounts well for the observations, in the 3 and 4 images experiments, of a nearly constant error-rate on all but the last image, and for a gradual increase of the error-rate on the last image. The situation is somewhat paradoxical, because if we reason in terms of a steady-state, we expect the fourth image to take the place of the third, the third to take the place of the second, and the second to take the place of the first. The results go clearly against such a steady-state view of memory, at least in the block-trial experiments. In experiments on monkey's working memory, the animals had to attend a continuous stream stream of images, and react when they recognized an image that had been presented previously N steps back (Yakovlev et al., 2005). Memory might well work under steady-state conditions in these experiments.

If my structural interpretations are taken literally, the memory traces must migrate from one location to another. It is common to speak, in the multi-store memory models, of information being transferred from one store to another. In a depiction of such statements, one imagines some neuronal module, in a store, encoding some information through the state of activation of its synapses, and some other neuronal module, copying or translating this information, through modifications of its own synapses. Then, we are led to think about neuronal mechanisms for copying or translating information and ask whether or not there may be smart neuronal chips for performing such tasks. Actually, the concept of "neuronal copying" is found, in disguise, in the field of stereoscopic vision. The task there is to compare two nearly identical images, and one way to do so, in theory, is to translate one image over the other in search of the best local matches. Indirect psychophysical results have been interpreted in terms of a neuronal superimposition mechanism (Anderson and van Essen, 1987). Perhaps then, the major implication of our results is that memory – as distinguished from learning – might well make use of a neuronal copying mechanism.

## 7. The decision curve

When an enzyme deals with a correct substrate, in molecular biology, it spends a certain average processing time with it, the interaction being productive or not. When it interacts with an analog, there is also a processing time, and there is absolutely no theoretical relationship between the two processing times. The situation has been extensively studied in the case of messenger RNA translation on the ribosome. In early studies, it was found, based upon very crude analyses of the data, that processing times were extremely large in the case of incorrect associations of a ribosome with a non-cognate tRNA (Rodnina et al., 1996), and from there it was deduced that such non-cognate interactions were the limiting factor, in the rate of protein synthesis. This belief was incorporated into a logistic model of protein synthesis (Zouridis and Hatzimanikatis, 2008). More refined experiments eliminated the hypothesis of a bottleneck due to the non-cognate interactions, and proposed instead that there was a bottleneck due to the "near-cognate" interactions, those in which the ribosome interacted with a transfer RNA molecule having an anticodon rather similar to the anticodon of the cognate transfer RNA. The resulting kinetic model of protein synthesis (Gromadski and Rodnina, 2004) has been widely accepted until recently, and was incorporated into logistic models of protein synthesis (Fluitt et al., 2007). However, recent data suggest that the ribosome spends most of its time in processing correct interactions (Spencer et al., 2012).

In many psychophysical experiments, when there is a speed/accuracy tradeoff, it is reported that RT's for errors are usually smaller than RT's for correct responses (e.g., Ratcliff and Smith, 2004). This can be rationalized by the notion that hasty judgments are less reliable than mature ones.

---

Insert Figure 12 about here

---

On the other hand, RT's are substantially higher for the erroneous responses in my working memory experiments . When the subject has well memorized the image, he/she makes a rapid and correct response. Otherwise, he/she keeps searching for faint clues in memory. If the subject cannot decide, he/she makes a key press at random, in agreement with an alternative forced choice (AFC) procedure. Errors are mostly of this type. Large RTs should reflect the subject's uncertainty. So one expects that the less certain the subject is, the higher the error-rate. Actually, I expected the error-rate to increase steadily with RTs, and reach asymptotically the 50% level. The histograms in Fig. 12 show that RT distribution for errors are shifted to the right with respect to those for correct responses. This makes sense. The subjects are behaving responsibly. They respond rapidly when they know the answer, otherwise they make an effort to get more information from memory. What is quite unexpected, on the other hand, is the relationship between the tails of the distributions. As a matter of fact, the erroneous/total responses ratio is around 25 to 30% at the largest RTs, thus substantially lower than the expected 50% (Fig. 12). This finding must have profound implications. I found similarly an $< 50\%$ ceiling in data on learning visual patterns in baboons from Fagot and Cook, 2006. and similar work on a human being in Voss, 2009.

## 8. Recognizing a memorized image after black/white reversals

---

Insert Figure 13 about here

---

When an image is very simple (for instance, it is just showing the letter A), it will be recognized easily even after reversing the black and white values. On the other hand, complex images are less easy to recognize after reversing the black and white, values, as one can realize when trying to interpret landscapes or faces on film negatives. Jean-François Patri and I performed experiments on 5x5 images memorized then tested either in their original black and white version, or after an inversion of black and white, as illustrated in Fig. 13 (Patri and Ninio, 2009). The analysis of the RT distributions suggested that a simple two-steps scheme accounted for the RT distributions when tests used the normal contrast. When the tests involved the opposite contrast, the RT distributions could be interpreted as due to the superimposition of two pathways : the previous pathway in 25% of the cases, and a pathway involving one more step in 75% of the cases. The natural interpretation is that in 25% of the cases, a mental inversion of contrast is not needed to recognize the correct image in the test while in 75% of the cases, a mental inversion is needed, and it consumes just one elementary step. Here, I have completed the work by testing myself on 4x4 and 6x6 images. The results are shown in Fig. 14. In both cases, when the test images are shown with the normal contrast, the RT distributions are compatible with a two-step model, but in the case of presentations with black and white reversals, the RT distributions are modeled with the branched scheme of Fig. 1 e.

---

Insert Figure 14 about here

---

## 9. Recognizing a memorized image alone, or side by side with a distractor

In almost all my visual memory experiments, there were two images in the recognition tests (see Fig. 9). It was thought that showing the correct image side by side with a distractor would make recognition easier. An alternative procedure is to present a single image, and let the subject decide wether it is the correct one or not. In the first situation, the distractor may interfere with the stored items in memory and cause recognition errors, or it may be easily rejected if it contains an obvious feature that cannot be in the memorized image ; in the second situation one may feel uneasy, being unable to decide whether the image shown in the recognition test is exactly the memorized image, or some similar one. A comparison of the two procedures was undertaken in collaboration with Jean-François Patri, involving 10,000 tests on 5x5 images. In the presence of a distractor, errors were slightly lower, RTs were higher and the RT distributions were much flatter. The widening of the RT distributions, in the presence of the distractor can be explained by the need to represent two images instead of one, and the time spent in comparing the two images. I have repeated here the experiments using 4x4 images. All three RT distributions

can be simulated with a 2-steps model (Fig. 15). Errors are mostly observed in the absence of a distractor, when the incorrect image is presented in the test (i.e., errors are false positives).

---

Insert Figure 15 about here

---

## 10. Alternation frequencies in stereo vision

Most studies in stereo vision make use of error-rate arguments and rarely of RT arguments. However, in one case at least there was a study on RT distributions, supporting a fusion theory against a suppression theory of binocular vision (O'Shea, 1987). I deal here with a promising line of chronometric research, in which the two members of a stereoscopic pair are presented in alternation to the two eyes.

In normal early vision, the brain receives at least four streams of visual inputs. From each eye, the optic nerve splits at the level of the lateral geniculate nucleus and travels toward the primary visual cortex. A single conscious representation is constructed from the four data flows, and this raises problems of synchronization that have been addressed in a large number of chonometric experiments. Thus, in the well-known Pulfrich phenomenon, an attenuating filter positioned in front of one eye creates a very slight delay in the processing of the visual streams from that eye. When a moving target is attended, the information provided by the left eye on the target's current position is combined with the information provided by the right eye on the target's position slightly earlier. There is thus an apparent disparity that creates a stereoscopic depth effect. This phenomenon has been used as a tool to dissect in a refined way some temporal aspects of early visual processing (Read and Cummings, 2007).

Several chronometric problems arise when we try to understand how a 3d interpretation is constructed from the visual information sent by the two eyes, and in particular, how long the brain needs to carry out the stereoscopic calculations. Experimentally, the protocols of cyclic alternating presentations are promising. The left and right images of a stereoscopic pair are sent in alternation to the left and the right eye, and the cycles are repeated until a 3d interpretation eventually emerges. In some studies (e.g., Ogle, 1963), the left and right components are separated by a void interval. In other studies (e.g., Efron, 1957; Engel, 1970), the durations of the left and right presentation phases are varied independently. All authors agree with the fact that stereopsis needs several cycles to develop whenever an alternation protocol is used. Thus, stereopsis is not completed in one cycle. This suggests that partial computations may be accomplished during one cycle, and their result be somewhat kept in memory and used during the next cycle, at which further computations would be carried out. Typically, if we send stereoscopic images alternately to the two eyes, in a cyclic manner, stereopsis occurs at or above 1 Hz full-cycle frequencies for very simple stimuli. In this case the inputs to each eye may last 500 ms. With more complex stimuli, such as random-dot stereograms, higher alternation frequencies are required (Ludwig, Pieper and Lachnit, 2007).

The current explanation for stereopsis from temporally separated images is that (i) each stimulus leaves a trace during its presentation time plus a persistence time and that (ii) if the presentation plus persistence times of the two images presented in alternation overlap, stereoscopic calculations may be performed during this overlap period (e.g., Ogle, 1963; Engel, 1970). Rychkova and I determined, for 20 stereoscopic pairs that involved various types of computational difficulties (slant, curvature, camouflage, depth segregation, shape complexity, absence of shear disparities) the threshold alternation frequency at which stereopsis became possible. We thus established a hierarchy of the computational difficulties that could arise with various types of images. The threshold frequencies varied from 2.5 Hz, on average, for the simplest stimuli, composed of a few separate elements without slant or curvature, to 12.4 Hz for the most complex ones, random dot stereograms (Rychkova and Ninio, 2011). Difficult stereograms require high alternation frequencies. In this case, the left and right visual streams have short durations, but they have, apparently, a better opportunity to cooperate in the construction of the 3d representation. I am not aware of a quantitative or semi-quantitative model that would capture this phenomenology. Possibly, during the construction of the 3d percept, the loss of information due to natural decay of the stimuli traces is strongly dependent upon the nature of the stimulus. So, the more complex a stimulus, the more the decay must be compensated by refreshes of visual input.

---

Insert Figure 16 about here

---

In order to obtain more detailed information on the temporal aspects of stereoscopic interpretation with various stimuli, we extended our previous work by intercalating either (i) variable void intervals between the monocular presentation times or (ii) variable binocular intervals . In this way, a presentation cycle involved the presentation of one image to the left eye, then an interval in which both images were presented (or none), then the presentation of the other image to the right eye, then again a binocular or void interval. The use of intercalated binocular intervals produced important, unexpected results. We found that increasing the binocular interval by a certain amount made it possible to increase the monocular intervals by a much larger amount, without disrupting 3d perception (Rychkova, Rabitchev and Ninio, 2010). This suggests that the information that is acquired during truly binocular presentations might be more reliable and less subject to decay than the information acquired during the persistence overlap period (Fig. 16). There is however a complication. Assume that a binocular interval is sufficiently long to allow by itself the emergence of a 3d interpretation. It is then followed by a monocular presentation to the left or the right eye. If the monocular interval is short enough, the 3d percept persists, as in the case of strictly alternating monocular inputs. On the other hand, If the monocular interval is too long, it becomes obvious to the brain that there is no longer evidence for binocular information, so the 3d interpretation collapses. This is observed for large enough monocular intervals, and the subject experiences a regime of “pulsating stereopsis”, an alternation between 3d and 2d interpretations, as shown by the crosses in Fig. 16. S. Rychkova and I speculate that there is also an intermediate range of binocular intervals in which the subject should experience

pulsating stereopsis, yet reports stable stereopsis, suggesting that he/she is "blind" to the discontinuous character of 3d perception in this range. This would happen in the triangular domain above the dotted line in Fig. 16.

In the case of these experiments, one may speak of "inverse" chronometry, as for the experiments described in Fig. 7. The presentation times are predetermined, and we determine the subject's response as a function of the presentation times. What we hope, in the long term, is to derive a model of the time-course of the construction of a 3d interpretation by the brain. At present, there are too many parameters to feed the models, and not enough details in the experimental results. To elaborate such a model, we would like to have experimental results indicating how many alternating presentations are needed for the emergence of a 3d interpretation.

## 11. Discussion

In molecular biology, there is an abundance of kinetic models such as those of Fig. 1, and even more complex ones, but the data describing the whole distribution of processing times, from enzyme substrate docking to product release cannot match the fine details of the models. Prior to the era of single molecule studies, the fast kinetic experiments were performed on large ensembles of molecules, there were problems of synchronization, and problems of heterogeneities in the time scales of the different steps in the reactions. With the advent of optical tweezers and FRET techniques, it became possible to study the details of molecular events on large macromolecules, for instance the progression of RNA polymerases on DNA molecules being transcribed (e.g., Eid et al., 2009, Fig. S1 of their Supporting Material) or the processing of transfer RNA molecules on the ribosome (Geggier et al. 2010). Still there are problems of multiplicity of conformational states at each stage, and multiplicity of reaction pathways (review in Zhuang, 2005). Furthermore, it is difficult to obtain data in the short time range (milliseconds) where they might best discriminate between models.

In several domains of visual psychophysics in which I invested myself (visual illusions, stereo vision, visual memory) the general trend was to determine error levels, and pay little attention to reaction times, but there were exceptions, such as the famous studies of Sternberg, 1966 on "high-speed scanning in memory" and of Shepard and Metzler, 1971 on "mental rotations". In my own work, I focused initially on error levels, but measured reaction times routinely, as supplementary information. Contrary to many colleagues who liked to perform experiments at high error-levels – as a matter of fact, under the conditions of "just noticeable differences", I preferred to work under low error-level conditions, in which the subject feels at ease with the tests. Typically, in the visual memory work, I try not to exceed the 15% error levels. It turns out that RTs provide more precise information than error levels. Let us assume that in a certain type of test there are 100 errors for 1000 measurements. This value of 100 is then determined with a ± 10 % uncertainty. Let us assume that the mean RT is one second, and the standard deviation is typically 0.3 sec. Then, the mean is reliable ± 0.3/(square root of 1000) = 9.5 ms!

Having very large data sets (over 300,000 RTs in Ninio, 2004) it was tempting to look into RT distributions. At the beginning, I was satisfied with the fact that histograms from pooled data (Fig. 2 in Ninio, 2004, reproduced here in Fig. 12) were well-modeled with lognormal distributions. It was also clear that in easy situations (when a recognition

test followed immediately the presentation of an image) the RT distributions could be very sharp, and that they became progressively wider as the complexity of the task increased.

Most RT distributions in our visual memory studies, and also in other tasks relevant to neurophysiology (for instance visuomotor tasks) share common features : there is a dissymmetrical bell-shaped curve that rises steeply after a lag, then declines slowly. Numerous models to predict such a shape, were shown to make a good fit to the experimental data, within the limited accuracy and caveats of psychophysical experiments, including the ex-Gaussian, the gamma, the lognormal, or the Weibull distributions (e.g., Matzke and Wagenmakers, 2009; Ulrich and Miller, 1993; McGill and Gibbon, 1965; Colonius, 1995).

The kinetic modeling inspired by molecular biology invited itself naturally in a work with a limited ambition, carried out in collaboration with Jean-François Patri. We wondered how easy it would be to recognize a memorized image, when the test involved the "negatives" of the image and its distractor (i.e., the images after an inversion of the black and white values). In a recognition test, the brain may recognize at once some memorized shapes, whether they are presented with their original or their inverted black and white values. In other cases, the brain may need to perform a "mental inversion of contrast" to recognize the memorized image. Therefore, there would be two recognition pathways, the direct one, and an indirect one involving mental inversion of contrast. There would be a wiring diagram such as that of the (e) model "with a branchpoint" of Fig. 1. We determined that under the conditions of our experiments, 25% of the decisions could follow the standard simple path, and 75% of the decisions could require an additional step of mental inversion of contrast (Patri and Ninio, 2009).

The simplicity and reasonable character of this result encouraged me to pay even more attention to RT distributions. In a study on symmetry perception, I compared the RT distributions for comparing images side by side to the RT distributions for comparing images related by a symmetry axis, more precisely, I compared RTs for symmetry violations to RTs for repetition violations. At the lowest studied complexities (3x3 images), the RT distribution for symmetry violation was well modeled by an ex-Gaussian + a shift.

The ex-Gaussian is well known and frequently found in mental chronometry studies. It is the result of the convolution of an exponential decay – the "one step" kinetic model of Fig. 1 – with a Gaussian that widens the RT distribution and replaces the vertical initial rise by a steep but smooth initial rise. Here, it applies well to the 3 RT distributions shown in Fig. 4 (top and bottom left) and 6 (top left). In 12 other cases, the RT distributions were wider and could be modeled with a "two-step" kinetic model + shift, convoluted with a Gaussian. Therefore, we had a natural extension of the ex-Gaussian distribution : the exponential decay that formed the kinetic core of this distribution was replaced by a slightly more complex kinetic core formed of two successive exponential decays. This review shows that many RT distributions in visual memory studies can be modeled with the combination of a kinetic core, a Gaussian widening factor, and a shift.

General models for RT distributions in mental processes have been proposed earlier, based upon theories on how decisions are taken, the most famous ones being the random walk models (e.g., Pike, 1973 ; Ratcliff, 1978) and the accumulator model (Vickers, 1970), and there are also models rooted on neurophysiological processes (e.g., Norwich and Wong, 1995 ; Medina, 2012). The failures and successes of a number of

models have been discussed in Luce's classical book (Luce, 1986) as well as in a number of more recent articles (e.g., Van Zandt et al., 2000; Miller and Ulrich, 2003; Ratcliff and Smith, 2004; Schmiedek et al., 2007). Medina (2012) made a connection between a class of psychophysical models, embodied in Piéron's law, and Michaelis kinetics in enzymology. According to Ratcliff and Smith, 2004 “Although none of the models we evaluate mimics another exactly, we show that some can mimic each other sufficiently to render them, for all practical purposes, empirically indistinguishable”. They also state, in the same article, that RTs on errors are generally lower than RTs on correct responses. Quoting earlier work, Van Zandt et al., (2000) state that in general, but not always, the RTs are smaller for the “same” than for the “different” responses.

I used kinetic modeling because I had already an interactive computer graphics program suited for it (I used it to check enzymological results), but do not claim that it is more realistic than alternative models. On the other hand, I am struck by several facts. The data bases upon which other models were devised differ substantially from my data base on visual memory. In my case, the “same” judgments take more time, in general, than the “different“ judgments, and RTs on errors are larger than RTs on correct responses. These two differences are probably related to the fact that most publications on RT distributions deal with situations in which the subject responds to rather simple stimuli, but presented at near threshold detectability, whereas in my case, I deal with complex but highly visible stimuli.

The fact that the predictions of one model may be mimicked by the predictions of another model is a general feature in scientific work. As Koenderink (2002) puts it very elegantly, “there exist many trivial tricks to make a theory fit the facts that are a little better than cosmetics”. So, is my kinetic modeling better than cosmetics?

The kinetic modeling has at least the merit of being very flexible. With a starting state S, a resulting final state R and zero to three intermediates, I was able to model the 21 histograms shown in this review. When a reversibility is introduced between two states, time is spent going back and forth between the two states, and this widens and flattens the RT distributions. (as in the side by side comparisons of Fig. 4, right panels). When a branchpoint is introduced, we have a superimposition of two pathways, that may account for bimodality in the histograms (see for instance Fig. 6, bottom right panel and Fig. 14. right panels). Nonetheless, there are also limitations in kinetic modeling. Here, all models in Fig. 1 have a unique starting point S. Introducing a branchpoint as in (e) or (f) of Fig. 1 is not as radical as accepting the existence of two or several starting points. This situation arises in classical enzymology, when the starting preparation is a heterogeneous mixture of non-interconvertible enzymes. But what can the brain's analog of non-interconvertible states be?

The core elementary step – the exponential decay – cannot be entirely correct, when one considers enzymatic steps that require large relative movements of the substrate and the enzyme. Diffusive steps should then be taken into account, and these are not reducible to finite successions of exponential decays. So, there is room for a refinement of the elementary step in the context of mental chronometric studies. Here, we played with the “wiring diagram” of the core kinetic scheme. Other authors, dealing with complex situations, may use wiring diagrams similar to ours, but replace one or more kinetic steps by what they believe to be more pertinent modules (e.g., accumulators, random-walks, etc.).

Are the kinetic models physiologically pertinent ? I have no reason to trust or not to trust exponential decays as basic modules in the neural network activities subtending perceptual decisions. I am struck by the fact that some RT distributions may be very sharp (for instance, the distribution for symmetry violations in 3x3 image comparisons). I am also conscious of the fact that some experimental distributions owe their wideness to many sources of heterogeneity. Many subjects may have contributed to the data (here, this source of heterogeneity was limited by taking myself as unique subject in most reported experiments – however, my level of arousal could not be kept constant during the experiments). The stimuli can be extremely heterogeneous. Clearly, images with very fragmented shapes are more difficult to deal with than images that contain a few blocks of black or white shapes. An image may be very fragmented in one version, and look very simple upon a black/white inversion. This aspect of shape perception deserves being investigated. Also, in many cases, there is no positive recognition of the test image, and the decision is based upon a rejection of a distractor that looks clearly unfamiliar. There are also some (almost hidden) sources of heterogeneity. For instance, I have some systematic inequalities in RTs and errors-rates in recognition tests, depending on whether the distractor is on the left or on the right. Therefore, in my opinion, kinetic models cannot be taken too literally. They are mainly a way to explore the relationships within a series of experimental RT distributions, by putting the finger on hypothetical changes in the wiring diagrams.

In this work, reasonably smooth and detailed histograms required around 7,000 data points. Roughly, two hours of testing in front of a monitor are needed to acquire 1000 RTs in visual memory tests, so the data partially reported in Fig. 4 required > 100 hours of testing – and those in Ninio, 2004, about 600 hours of testing. This is a small amount of work, in relation to the enormous theoretical implications, and compared to the amount of work required in other domains (for instance, the years of tedious work by whole teams to establish crystallographic structures of proteins even in the 1980's). However, it seems that in the domain of psychophysics, the standard experiment makes use of about 40 hours of testing in front of a computer screen, and there is no tradition of high precision results.

Last, I am aware of the fact that a technological breakthrough may be the best complement or substitute to the modeling work. Eye movements studies are sorely needed in the side by side visual comparison work (but none of my colleagues in France having access to eye movements measurements found the topic interesting enough for a collaboration). Brain imaging studies might help to detect intermediate states preceding the final responses, thus would help to clarify the wiring diagrams postulated in the kinetic models.

## Appendix: kinetic modeling of RT distributions

The kinetic formalism (Fig. 1) is extremely classical, it has been expounded in numerous textbooks (e.g., Cornish-Bowden, 2012). Here, it is adapted with some modifications to the visual memory experiments. Following a first discussion, with appropriate references, in the appendix to Ninio (2011), I give here, more explicitly, the modeling algorithm I use . The time-course of a reaction, in a kinetic scheme involving N states is obtained by writing, for each state, the losses and the gains during an infinitesimal slice of time dt. For a given compound or state A, the losses are those represented by the arrows from state A

to its immediate neighbors, and the gains are those represented by the arrows to A from its immediate neighbors. For instance, in the case of scheme f of Fig. 1, involving 5 states, including the starting state S and the terminal state R, we write – the concentration of a compound being designated by the name of the compound within square brackets :

$$d[S]/dt = -k_1 [S] + k_{-1} [I1]$$

$$d[I1]/dt = k_1 [S] - [k_{-1} + k_2 + k_3 ][I1] + k_{-2} [I2] + k_{-3} [I3]$$

$$d[I2]/dt = k_2 [I1] - (k_{-2} + k_4 )[I2]$$

$$d[I3/dt] = k_3 [I1] - (k_{-3} + k_5)[I3]$$

$$d[R]/dt = k_4 [I2] + k_5 [I3]$$

First step : The evolutions of the concentrations of all the compounds are followed, in my simulations, by using time slices dt = 5 milliseconds in the case of narrow histograms, or dt = 10 milliseconds in the case of wider ones, and updating all the concentrations according to the above equations. Initially, [S] = 1, and all other states are set to 0. The process terminates when the terminal states are completely filled (here, there is a single terminal state R). So, we follow R1(t), the accumulation of R over time.

Second step : we add to each value R1(t) the chosen value for the lag, giving a function R2(t) = R1(t -lag), for t > lag, and 0 otherwise.

Third step : we convolute the function R2(t) with a Gaussian of unit surface, and of variance sigma square. In practice, we take a centered Gaussian G(T) of unit surface, defined as above in steps of 5 or 10 milliseconds, and move it along the abscissa axis to form the convolution product with R2(t) = integral over all values of T, of G(T)R2(t + T).

Here, there is a single terminal state R. There is no leakage, while in enzyme kinetics, the reaction may terminate with an abortion : so, the arrows with kinetic constant $k_{-1}$ usually mean there « release of the substrate ». I also stress here that when the scheme starts with a reversible step (as in models c, d, and f of Fig. 1) the back-reaction with the associated kinetic constant $k_{-1}$ counts as a terminal dissociation in enzyme kinetics, whereas it counts here as a recycling step, followed by a reinitiation.

The fit between the experimental histograms and kinetic models is quite easy. I have written an interactive computer graphics program that can be fed with histograms and any general kinetic model. The values of the kinetic parameters, the gaussian widening and the shift can be changed interactively, until the predicted RT distribution matches the histogram. This program written in C++ and OpenGL computer graphics runs well on the Linux operating system, and can be sent upon request.

## Acknowledgements

The “Laboratoire de Physique Statistique” (LPS), Ecole Normale Supérieure, is a “mixed research unit” (UMR 8550) of the CNRS associated to Paris 6 and Paris7 universities. I thank Jean-Pierre Nadal and the LPS for their unfailing support during nearly 25 years. I also thank Joel Fagot and Joel Voss for communicating their data published in Fagot and Cook, 2006, and Voss, 2009.

## References


Anderson, C.H., and van Essen, D.C. (1987). Shifter circuits: A computational strategy for dynamic aspects of visual processing. *Proc. Nat. Acad. Sci. U.S.A.* 84, 6297-6301.

Binet, A. (1894). *Psychologie des grands calculateurs et joueurs d'échec*. (Paris, Hachette)

Bogacz, R., Wagenmakers, E.-J., Forstmann, B. U., and Nieuwenhuis, S. (2009). The neural basis of the speed-accuracy tradeoff. *Trends in Neurosciences* 33, 10-16.

Bruce, V., and Morgan, M. (1975). Violations of symmetry and repetition in visual patterns. *Perception* 4, 230-249.

Brunel, N., and Ninio, J. (1997). Time to detect the difference between two images presented side by side. *Cognitve Brain Research* 5, 273-282.

Colonius, H. (1995). The instance theory of automaticity : Why the Weibull ? *Psychological Review* 102, 744-750.

Corballis, M.C., and Beale, I.L. (1971). On telling left from right. *Scientific American* 224(3), 96-104.

Cornish-Bowden, A. (2012) Fundamentals of Enzyme Kinetics. 4th edition, Weinheim: Wiley-Blackwell.

Drake, J.W., Charlesworth, B., Charlesworth, D., and Crow, J.F. (1998). Rates of spontaneous mutation. Genetics 148, 1667-1686.

Efron, R. (1957). Stereoscopic vision: 1, Effect of binocular temporal summation. *British Journal of Ophthalmology* 41, 709-730.

Eid, J., Fehr, A., Gray, J., Luong, K., Lyle, J., et al. (2009) Real-time DNA sequencing from single polymerase molecules. Science 323, 133-138.

Elez, M., Murray, A.W., Bi, L.-J., Zhang, X.-E., Matic, I., and Radman, M. (2010). Seeing mutations in living cells. Current Biology 20, 1432-1437.

Engel, G.R. (1970). An investigation of visual responses to brief stereoscopic stimuli. *Quarterly Journal of Experimental Psychology* 22, 148-166.

Fagot, J., and Cook, R.G. (2006). Evidence for large long-term memory capacities in baboons and pigeons and its implications for learning and the evolution of cognition. *Proc. Nat. Acad. Sci. U.S.A.* 103, 17564-17567.

Fischer, E. (1894). Einfluss der Configuration auf die Wirkung der Enzyme [influence of configuration on the action of enzymes] *Berichte der Deutschen chemischen Gesellschaft zu Berlin* 27, 2985-2993.

Fluitt, A., Pinaar, E., and Viljoen, H. (2007). Ribosome kinetics and aa-tRNA competition determine rate and fidelity of peptide synthesis. *Computational Biology and Chemistry* 31, 335-346.

1158 Geggier, P., Dave, R., Feldman, M.B., Terryl, D.S., Altman, R.B., Munro, J.B., and
1159 Blanchard, S.C. (2010). Conformational sampling of aminoacyl-tRNA during selection on
1160 the bacterial ribosome. *Journal of Molecular Biology* 399, 576-595.

1161 Gorini, L. (1971). Ribosomal discrimination of tRNAs. *Nature New Biol.* 234, 261-264.

1162 Gromadski, K.B., and Rodnina, M. (2004). Kinetic determinants of high fidelity tRNA
1163 discrimination on the ribosome. *Molecular Cell* 13, 191-200.

1164 Harris, C.M., Waddington, J., Biscione, V., and Manzi, S. (2014). Manual choice reaction
1165 times in the rate-domain. Frontiers in Human Neuroscience 8, article 418. doi:
1166 10.3389/fnhum.2014.00418

1167 Hopfield, J.J. (1974). Kinetic proofreading: a new mechanism for reducing errors in
1168 biosynthetic processes requiring high specificity. *Proc. Nat. Acad. Sci. U.S.A.* 71, 4135-
1169 4139.

1170 Hopfield, J.J. (1980). The energy relay: A proofreading scheme based on dynamic
1171 cooperativity and lacking all characteristic symptoms of kinetic proofreading in DNA
1172 replication and protein synthesis. *Proc. Nat. Acad. Sci. U.S.A.* 77, 5248-5252.

1173 Koenderink, J.J. (2002). The head and the hands. *Perception* 31, 517-520.

1174 Köhler, W. (1918). Nachweis einfacher Strukturfunktionen beim Schimpansen und beim
1175 Haushuhn. Über eine neue Methode zur Untersuchung des bunten Farbensystems.
1176 *Abhandlungen der Königlich Preussischen Akademie der Wissenschaften, phys-math., KL*,
1177 pp. 3-4, 10, 12-13, 33.

1178 Kong, A., Frigge, M.L., Masson, G., Besenbacher, S., Sulem, P., et al. (2012) Rate of *de*
1179 *novo* mutations, father's age, and disease risk. Nature 488, 471-475.

1180 Luce, R.D. (1986). Response times : Their rôle in inferring elementary mental organization.
1181 Oxford : Oxford University Press.

1182 Ludwig I., Pieper W., and Lachnit H. (2007). Temporal integration of monocular images
1183 separated in time: stereopsis, stereoacuity, and binocular luster. *Perception &*
1184 *Psychophysics* 69*,* 92-102

1185 Mach, E. (1865). Über die Wirkung der raümlichen Verteilung des Lichtreizes auf die
1186 Netzhaut. 1, *Akademie der Wissenschaften in Wien, Sitzungsberichte, math.-nat. CL* 52,
1187 303-322.

1188 McGill, W.J. and Gibbon, W.J. (1965) The general gamma distribution and reaction
1189 times. *Journal of Mathematical Psychology* 2, 1-18.

1190 McKeithan, T.W. (1995). Kinetic proofreading in T-cell receptor signal transduction.
1191 *Proc. Nat. Acad. Sci. U.S.A.* 92, 5042-5046.

1192 Matzke, D., and Wagenmakers, E.-J. (2009). Psychological interpretation of the ex-
1193 Gaussian and shifted Wald parameters: A diffusion model analysis. *Psychonomic Bulletin*
1194 *& Review* 16, 798-817.

1195 Medina, J. M. (2012). Multiplicative processes and power laws in human reaction times
1196 derived from hyperbolic functions. *Physics Letters A* 376, 1617-1623.

Miller, J., and Ulrich, R. (2003). Simple reaction time and statistical facilitation : A parallel grains model. *Cognitive Psychology* 46, 101 – 151.

Nimi, R., Watanabe, K., and Yokosawa, K. (2005). The role of visible persistence for perception of visual bilateral symmetry. *Japanese Psychological Research* 47, 262-270.

Ninio, J. (1974). A semi-quantitative treatment of missense and nonsense suppression in the strA and ram ribosomal mutants of *Escherichia coli* . Evaluation of some molecular parameters of translation *in vivo*. *Journal of Molecular Biology* 84, 297-313.

Ninio, J. (1975). Kinetic amplification of enzyme discrimination. *Biochimie* 57, 587-595.

Ninio, J. (1977). Are further kinetic amplification schemes possible? *Biochimie* 59, 759-760.

Ninio, J. (1979). An algorithm that generates a large number of geometrical visual illusions. *Journal of Theoretical Biology* 79, 167-201.

Ninio, J. (1987). Alternative to the steady-state method: Derivation of reaction rates from first passage times and pathway probabilities. *Proc. Nat. Acad. Sci. U.S.A.* 84, 663-667.

Ninio, J. (1997). The evolutionary design of error-rates, and the fast fixation enigma. *Origins of Life and evolution of the biosphere* 27, 609-621.

Ninio, J. (1998). Acquisition of shape information in working memory, as a function of viewing time and number of consecutive images : evidence for a succession of discrete storage classes. *Cognitive Brain Research* 7, 57-69.

Ninio, J. (2004). Testing sequence effects in visual memory: clues for a structural model. *Acta Psychologica* 116, 263-283.

Ninio, J. (2006). Multiple stages in codon-anticodon recognition : double-trigger mechanisms and geometric constraints. *Biochimie* 88, 963-992.

Ninio, J. (2007). Mental kinetics in visual memory. *Perception* 36 Supplement, 52.

Ninio, J. (2011). Folded sheet *versus* transparent sheet models for human symmetry judgements *Symmetry* 3, 503-523.

Ninio, J., and Amigorena, S. (2004). How B cells and dendritic cells may cooperate in antigen purification. *Journal of Theoretical Biology* 231, 309-317.

Norwich, K.H., and Wong, W. (1995). *Mathematical Biosciences* 125, 83-108.

Ogle K. N. (1963). Stereoscopic depth perception and exposure delay between images to the two eyes. *Journal of the Optical Society of America* 53, 1296-1304.

O'Shea, R.P.O. (1987). Chronometric analysis supports fusion rather than suppression theory of binocular vision. *Vision Research* 27, 781-791.

Patri, J.-F., and Ninio, J. (2009). Recognising random shapes with inverted contrast polarity. *Perception* 38 *Supplement* 178.

Phillips, W.A. (1974). On the distinction between sensory storage and short-term visual memory. *Perception and Psychophysics* 16, 283-290.

Phillips, W.A., and Christie, F.M. (1976). Components of visual memory. *Quarterly Journal of Experimental Psychology* 29, 117-133.

Piaget, J. (1974) *Adaptation vitale et psychologie de l'intelligence. Sélection organique et phénocopie*. Paris, Hermann.

Pike, R. (1973). Response latency models for signal detection. *Psychological Review* 80, 53-68.

Pflugshaupt, T., Nyffeler, T., von Wartburg, R., Wurtz, P., Lüthi, M., Hubl, D., Gutbrod, K., Juengling, D., Hess, C.W. and Müri, R.M. (2007). When left becomes right and vice versa: Mirrored vision after cerebral hypoxia. *Neuropsychologia* 45, 2078-2091.

Ratcliff, R. (1978). A theory of memory retrieval. *Psychological Review* 85, 59-108.

Ratcliff, R., and Smith, P.L. (2004). A comparison of sequential sampling models for two-choice reaction time. *Psychological review* 111, 333-367.

Read, J.C.A., and Cumming, B.G. (2005). Effect of interocular delay on disparity-selective V1 neurons: relationship to stereoacuity and the Pulfrich effect. *Journal of Neurophysiology* 94, 1541-1553.

Rodnina, M.V., Pape, T. Fricke, R., Kuhn, L., and Wintermeyer, W. (1996). Initial binding of the elongation factor Tu.GTP.aminoacyl-tRNA complex preceding codon recognition on the ribosome. *Journal of Biological Chemistry*. 271, 646-652.

Rychkova, S., and Ninio, J. (2011). Alternation frequency thresholds for stereopsis as a technique for exploring stereoscopic difficulties. *i-Perception* 2, 50-68.

Rychkova, S.I., Rabitchev, I.E., and Ninio, J. (2010). Stereoscopic memory beyond stimuli persistence: the multiplicative effect of binocular intervals. *Perception* 39 *Supplement* 161

Scott-Brown, K.C., Baker, M.R., and Orbach, H.S. (2000). Comparison blindness. *Visual cognition* 7, 253-267.

Shepard, R.N., and Metzler, J. (1971). Mental rotation of three-dimensional objects. *Science* 171, 701-703.

Schmiedek, F., Oberauer, K., Wilhelm, O., Süß, H.-M., and Wittmann, W. W. (2007). Individual differences in components of reaction time distributions and their relations to working memory and intelligence. *Journal of Experimental Psychology: General* 136, 414-429.

Spencer, P.S. , Siller, E., Anderson, J.F., and Barral, J.M. (2012). Silent substitutions predictably alter translation elongation rates and protein folding efficiencies. *Journal of Molecular Biology* 422, 328-335.

Sternberg, S. (1966). High speed scanning in human memory. *Science* 153, 652-654.

Tyler, C.W. (1996). *Human symmetry perception. In Human symmetry perception and its computational analysis* (Tyler, C.W., ed.), pp. 3-22. (Zeist, The Netherlands, VSP).

Ulrich, R. and Miller, J. (1993). Information processing models generating lognormally distributed reaction times. *Journal of Mathematical Psychology* 37*,* 513-525.

van der Vloed, G., Csatho, A., and van der Helm, P.A. (2007). Effects of asynchrony on symmetry perception. *Psychological Research* 71, 170-177.

Van Zandt, T., Colonius, H., and Proctor, R.W. (2000) A comparison of two response time models applied to perceptual matching. *Psychonomic Bulletin & Review* 7, 208 – 256.

Vickers, D. (1970). Evidence for an accumulator model of psychophysical discrimination. *Ergonomics* 13, 37-58.

Voss, J.L. (2009). Long-term associative memory capacity in man. *Psychonomic Bulletin & Review* 16, 1076-1081.

Wickelgren, W. A. (1977). Speed-accuracy tradeoff and information processing dynamics. *Acta Psychologica* 41, 67-85.

Wilding, J., and Valentine, E. (1997). *Superior memory*. (Hove, U.K., Psychology Press Ltd)

Winograd, S., and Cowan, J.D. (1963). *Reliable computation in the presence of noise*. (Cambridge, Mass., MIT Press).

Yakovlev, V., Bernachia, A., Orlov, T., Hochstein, S., and Amit, D. (2005). Multi-item working memory — A behavioral study. Cerebral Cortex 15, 602-615.

Zhuang, X. (2005). Single-molecule RNA science. *Annual Review in Biophysics and Biomolecular Structure* 34, 399-414.

Zouridis, H., and Hatzimanikatis, V. (2008). Effect of codon distributions and tRNA competition on protein translation. *Biophysical Journal* 95, 1018-1033.

## Fig. legends

**Fig. 1.** Examples of simple reaction schemes used here, and in enzyme kinetics. (a) the exponential decay, the most elementary scheme. The transition between the starting and final states occurs with a constant probability per unit time. The more complex reaction schemes (b) to (f) are all composed of such elementary steps. After convolution with a Gaussian, we get an ex-Gaussian RT distribution, and after the inclusion of a lag, we obtain a nice fit with the most narrow experimental distributions shown in Figs. 4 and 5. (b) scheme with two consecutive (irreversible) elementary steps. After inclusion of a lag and convolution with a Gaussian, we obtain a good fit with some of the experimental distributions shown in Figs 6, 12, 14, 15. (c) Classical Michaelis-Menten kinetics. Most experimental studies on enzyme kinetics are interpreted in terms of this scheme. More precisely, one assumes that a substrate binds to the enzyme, to form an intermediate complex I. This complex may either lead to the formation of the product, with the attached kinetic constant $k_2$, or dissociate abortively, with the kinetic constant $k_{-1}$. The sticking time of the enzyme-substrate complex is the reciprocal of $k_{-1}$, and the characteristic rate of transformation of the intermediate complex into the product is $k_2$. This scheme is all that is needed to establish an efficiency-accuracy tradeoff in enzyme-substrate interactions. Here, the scheme is used to model the RT distributions in Fig. 4, central panels. Introducing a reversible step widens the RT distribution, because it creates

many opportunities for back and forth motions between I ans S before the final transition to R. (d) A linear scheme with 4 compounds and 2 intermediate states that starts with two reversible steps. In this way, a still more important widening of the RT distributions is obtained. This scheme was used to model one of the RT distributions in Fig. 4. (e) A scheme with one branchpoint. This scheme was elaborated to model the results of the experiments in which, after memorizing an image, the subject is confronted with a recognition test in which the images are presented either in their normal contrast, or after an inversion between black and white (Fig. 13). So, there is a short pathway $S \rightarrow I1 \rightarrow R$ for the presentations with normal contrast, and a longer pathway involving a "mental flip" $I1 \rightarrow I3$ for the presentation with contrast inversion. This scheme was used to model the RT distributions of Fig. 14, right panels. (f) A still more complex scheme, with a branchpoint and three reversible steps. The scheme was used to model an RT distribution in Fig. 4.

**Fig. 2.** Stimuli used in image comparison studies. All the stimuli are generated over slightly distorted square grids. Black or white values are assigned at random to the quadrangles delimited by the grid. In most experiments, the grid is not drawn explicitly, allowing the black or white quadrangles to associate into continuous shapes of a single color. Images can be perceived as formed of black shapes over a white background, or as white shapes over a black background. First row: the task was to move a cursor on the screen, driven with a mouse, to the position of the difference, when it was located. In the left, I show a 10x10 pair of stimuli with a grid, and on the right, I show a pair of stimuli with the same pattern of black or white elements, but without grid. In the presence of a grid, the reaction times were on average higher by 20%. For $N \leq 9$, when the lattice was made irregular, performance did not deteriorate, up to a high level of irregularity. Furthermore the presence of uncorrelated distortions in the left and right images did not affect performance for $N \leq 6$ (Brunel and Ninio, 1997). In the central and bottom rows, I show stimuli that were used in experiments that involved a different paradigm: the left and right images of a pair, were either identical, or differed at a single position. The task was to indicate, with a left or right mouse button press whether the images were judged to be identical or to differ at a single position. The subject was not asked to locate the position of the difference. Reaction times and reaction time distributions are shown in Figs. 3 and 4.

**Fig. 3.** Mean reaction times in comparing images side by side. As the complexity of the images increase, from 2x2 to 8x8, the decision becomes comparatively longer when the images are the same. This is due to the fact that, in this case, the subject needs to perform a complete scanning of the two images before being convinced that there is no difference. With 2x2 images, the decision is faster (by 112 msec.) for the "same" comparison. For an explanation. see the legend to Fig. 4. The experiment was performed by the author. In this study, the tests were separated by a 1.0 s blank interval. Each data point represents the average RT over > 7,000 measurements. Similar results involving 8 subjects are shown in Brunel and Ninio, 1997, Fig. 5 or 18 other subjects in Ninio, 2011, Fig. 2, top right panel.

**Fig. 4.** Reaction time distributions in comparing 2x2, 4x4 or 6x6 images side by side. The mean reaction times are represented in Fig. 3. Each histogram represents at least 7,000 results. The bin width is 25 ms, except in the histograms for 6x6 images, where it is 50 ms. However, to harmonize the ordinate scales, each bin was treated as a pair of bins of 25 ms width. The histograms for the total RTs (correct + incorrect responses) are shown in gray, and the histograms for the erroneous responses are shown in black. The continuous curves represent simulations with models involving a kinetic core from Fig. 1, plus a lag and a Gaussian widening factor. Lag values from left to right, and top to bottom : 0.615 s, 0.8 s, 0.904 s, 0.535 s, 0.746 s, 0.95 s. Gaussian sigma : 0.7 s, 1.15 s, 0.75 s, 0.7 s, 1.2 s, 1.0 s. Kinetic cores : $k_1$ = 6.64/s and 6.32/s for the 2x2 different and same images respectively, $k_1$ = 3.06/s and 2.29/s for the 4x4 different and same images respectively, and $k_{-1}$ = 5.26/s and 1.22, $k_2$ = 15.5/s and 12.7/s. Kinetic core for the 6x6 different images : $k_1$ = 2.0/s, $k_{-1}$= 1.19/s, $k_2$ = 7.14/s, $k_{-2}$ = 12.2/s, $k_3$ = 13.4/s. Kinetic core for the 6x6 similar images : $k_1$ = 2.0/s, $k_{-1}$ = 0.70/s, $k_2$ and $k_3$ = 2.6/s, $k_{-2}$ and $k_{-3}$ = 10.0/s, $k_4$ and $k_5$ = 10.0/s. The slightly more rapid responses for the same versus the different responses in the case of 2x2 images (112 ms, on average) can be related to two factors : (i) the fact that the ”same” answer is made with a key press on the left of the mouse, while the different response involves a key press on the right of the mouse. This factor may account for an 80 ms difference in the lags. (ii) the $k_1$ in the kinetic core is also faster in the case of similar images. This might be a cognitive effect.

**Fig. 5.** Stimuli for the detection of symmetry violations. Here, pairs of 3x3, 4x4 or 5x5 symmetrical or nearly symmetrical images are juxtaposed along a vertical symmetry axis. The subject has to judge whether there is perfect symmetry or symmetry violation. The reaction times are significantly shorter and the RT distributions significantly narrower than in the case of repetition judgements (Ninio, 2011, and Fig. 6).

**Fig. 6.** The advantage of symmetry. (From Fig. 4 in Ninio, 2011). The experiments were performed by the author. 13,000 RTs were collected for the symmetry histograms, and 16,000 RTs were collected for the repetition histograms. The RT distributions are very significantly narrower, and the average RTs smaller in the case of symmetry judgments. The values for the lags, the Gaussian widenings, and the kinetic parameters of the kinetic cores are given in Ninio, 2011. Note that the histograms for the 5x5 repetition experiments seem to be made up of two components. This is indeed the case, and is seen when one separates the “same” from the “different” responses, as done here in Fig. 4.

**Fig. 7.** Time to memorize images of increasing complexities. (From Ninio, 1998). Left panel : data from Binet (1894) showing the time, given in abscissa to memorize the number of digits given in ordinate. Unfilled circles, performances by the prodigy calculator Diamandi who memorized the digits visually ; triangles, performances by the prodigy calculator Inaudi who had acoustic memory ; squares, performances by a mnemonist, Mr Arnould who recoded the lists of digits as letter strings. The straight lines, in this log-log plot correspond to a trend in $t^{0.58}$. Right panel : Memorizing images at long exposure times, given on a square-root scale. The experiments were performed by the author at an interval of 11 months. In the first experiment, the images were viewed for as long as seemed useful. The viewing time given in abscissa is the average for a series of

100 images of size 6x6 (black disks), 7x7 (unfilled circles), 8x8 (triangles), 10x10 (black square) or 12x12 (unfilled squares). There were 1400 images and 82 errors in all. The second experiment (unfilled diamonds) was performed after 11 months of intensive practice. Image sizes ranged from 6x6 to 12x12 and the viewing time was constant within each block of 100 images. In this experiment, 2400 images were viewed, and 590 errors were recorded. For both panels, the postulated 4 to 7 chunks limit of human short term memory is reflected by the rather small deviation close to the origin, with respect to the power law.

**Fig. 8.** Number of memorized bits on 8x8 images as a function of presentation times. (Data taken from Ninio, 1998). Here, the short presentation time domain (as compared to the range in **Fig. 6**) is explored. Left panel : results of two independent experiments. The first one involved 15 subjects, single images, and viewing times from 1 to 5 s (unfilled circles). The second experiment involved 14 subjects, and either single images (black disks) or two consecutive images tested in the same order (squares). Right panel : experiment performed by the author under similar conditions. The remarkable feature in the left panel is the absence of a noticeable increase in memorization, from 2 to 8 seconds presentation. In the right panel, the effect of training is not an improvement of purely visual memory, but an enhanced ability to detect pertinent patterns in the image (for instance, are there blocks of a same color, and do they touch each other?)

**Fig. 9**. The random testing protocol. Three images numbered 1, 2, 3 are presented successively for a constant duration, then followed by three recognition tests in any of the six possible orders. From Ninio, 2004, and here, Section 6 and Fig. 10.

**Fig. 10.** Dissociations between error-rates and RT patterns in memorizing three images, and testing them in random order. (Data taken from Ninio, 2004). Left panel: error-rate patterns. Results for a given image, tested at a given testing stage (indicated in abscissa) but belonging to different permutations (for instance, image 2 in testing permutations 123 and 321) were pooled. The horizontal segments indicate the total number of errors recorded for the image that labels the segment, at the given testing stage. The presentation times ranged from 1.65 to 1.9 sec, and the image sizes were, depending on the subject 6x5 or 5x5. The error-rate on the third image is very low when it is tested first. It increases at testing stages 2 and 3. On the other hand, the error-rates on the first and second images seem to be equal, and independent of the testing stage. It is conceivable that there are only 4 levels of storage accuracy detected in these experiments. Right panel : The reaction times for image i tested at rank $t > 1$ are split, in this representation, according to the image j tested at rank t-1. The horizontal bars indicate the values of the RTs, and the labels connected obliquely to the bars indicate the couple ji, j being in smaller type. The standard deviations indicated by the icon apply to $t > 1$. The RTs for image 3 at stage 1 is 0.508 s. The RTs were normalized in such a way that the average RT, in an experimental block of 90 images, excluding the “last in first out” cases, would be equal to one second.

**Fig. 11.** Model for visual working memory. (From Ninio, 2004). This minimal structure with seven slots A-G plus the STVM slot is proposed to account for the patterns of

reaction times inequalities observed in the 3 and 4 images experiments. After residing in STVM, the memory traces would move to A, then move upwards along the midline ACF and fill the rows by moving sideways. During recognition tests, the traces would move, if space permits, downwards from the EFG to the BCD row. One or two more rows would be required to account for the 5 images results. In this model, there are slots providing good quality of storage, located near the entrance (at the bottom), and slots providing less detailed storage, located at the back (on the top). An item, after being stored in STVM moves upwards to a lower quality store, then sideways to leave the passage free for the next memorized items. Now, and this is a crucial hypothesis, the item may also move downwards, if space permits, in which case, there is no further loss of information. So an item may migrate from slot to slot, following a complex path, loosing information when going upwards, and maintaining the information constant when going sideways or downwards.

**Fig. 12.** The decision curves. The two histograms represent data on RT distributions for recognition tests when 4 images are memorized then tested in random order (Fig. 2 in Ninio, 2004). The question addressed in Ninio, 2007 is that of the relation between the histograms for errors (in black) and the histograms for total RTs (in gray). The RTs were normalized in such a way that the average RT, in an experimental block of 90 images, excluding the "last in first out" cases, would be equal to one second. The left histogram was constructed from 35996 RT's and 3745 errors, the right histogram was constructed from 69390 RT's and 8892 errors. In the right panel, the error-rates are represented as a function of the progress in the histograms, for instance : first the time slice encompassing 0 to 6% of the total responses, then the time slice encompassing the 6% to 12% of the total RTs, then the time slice encompassing the 12% to 18% of the total RTs, etc. As expected, the response uncertainty, as measured by the error-level, increases when reaction times increase. On the other hand, even at the largest reaction times (the last time slice, up to 100% progression) the error-rate is clearly inferior to 50%, implying that there is still some valuable retrievable information in memory.

**Fig. 13.** Normal or inverted polarity of contrast? In this protocol, after memorizing an image, the subject is asked to identify it, either among a pair comprising this image and a distractor (second row) or a similar pair, but in which the black and white values were inverted (third row).

**Fig. 14.** Recognizing an image after an inversion of the polarity of contrast. Each histogram represents 7,500 to 7,600 RTs. As expected, the RTs are larger for the tests made in the inverted contrast mode. In this case, the models involve, logically, a branchpoint, expressing the choice made by the brain between looking at the images normally, or making a mental inversion between black and white. The parameters of the models, from left to right, and top to bottom were : lag; 0.56 s, 0.66 s, 0.63 s, 0.81 ; Gaussian sigma: 0.4 s, 1.05 s, 0.4 s, 1.3 s ; kinetic cores : $k_1$ = 3.1/s, 4.3/s, 2.2/s, 2.5/s ; $k_2$ : 22.6/s, 11.5/s, 11.6/s, 6.1/s and additionally, for the inverted contrast histograms, $k_3$ = 2.29/s, 1.0/s, $k_4$ and $k_5$, 16.0/s in both cases.

**Fig. 15.** Recognizing an image, in the absence or the presence of a distractor. After memorizing a 4x4 image, a test is made, either in the standard way (in the presence of a distractor) or with a single image, which can be the correct one (left histogram) or the incorrect one (central histogram). The parameters of the models, from left to right are : lag = 0.54 s, 0.59 s, 0.56 s ; Gaussian sigma : 0.5 s, 0.7 s, 0.4 s. Kinetic cores : $k_1$ = 3.8/s, 4.0/s, 3.0/s ; $k_2$ = 35.1/s, 27.5/s, 20.5/s.

**Fig. 16.** Stereo vision, with alternating presentations to the two eyes : A phase diagram. A complete presentation cycle involves the ”monocular” presentation of the left image of a stereo pair to the left eye, for a duration indicated in ordinate, then a void interval or a ”binocular” presentation of the two images, for a duration indicated in abscissa, then the monocular presentation of the right image to the right eye, then again a void or binocular presentation interval. Selecting a fixed, particular void or binocular interval, shown in abscissa, one determines the longest monocular duration that allows the occurrence of a correct 3d perception, shown in ordinate. An essential result of this study is that the intercalation of a moderate binocular interval between the left and right monocular presentation intervals (Phase 2) allows a much larger increase of their durations. At large binocular intervals (Phase 4), there is a first transition from stable stereopsis to pulsating stereopsis (lower curve) and a second transition from pulsating stereopsis to no stereopsis at all (upper curve). In Phase 3, the first transition is not observed experimentally, it is conjectured to occur in hidden form, as represented by the triangular blue domain. In this domain, the subjects actually report a single transition, from stable stereopsis to no stereopsis (upper curve). The continuity between the Phase 3 and Phase 4 upper curves suggests that stereopsis also has an interrupted character in the blue domain but the subjects are not conscious of the situation. The dashed segment is speculative, it makes the interpretations more coherent.

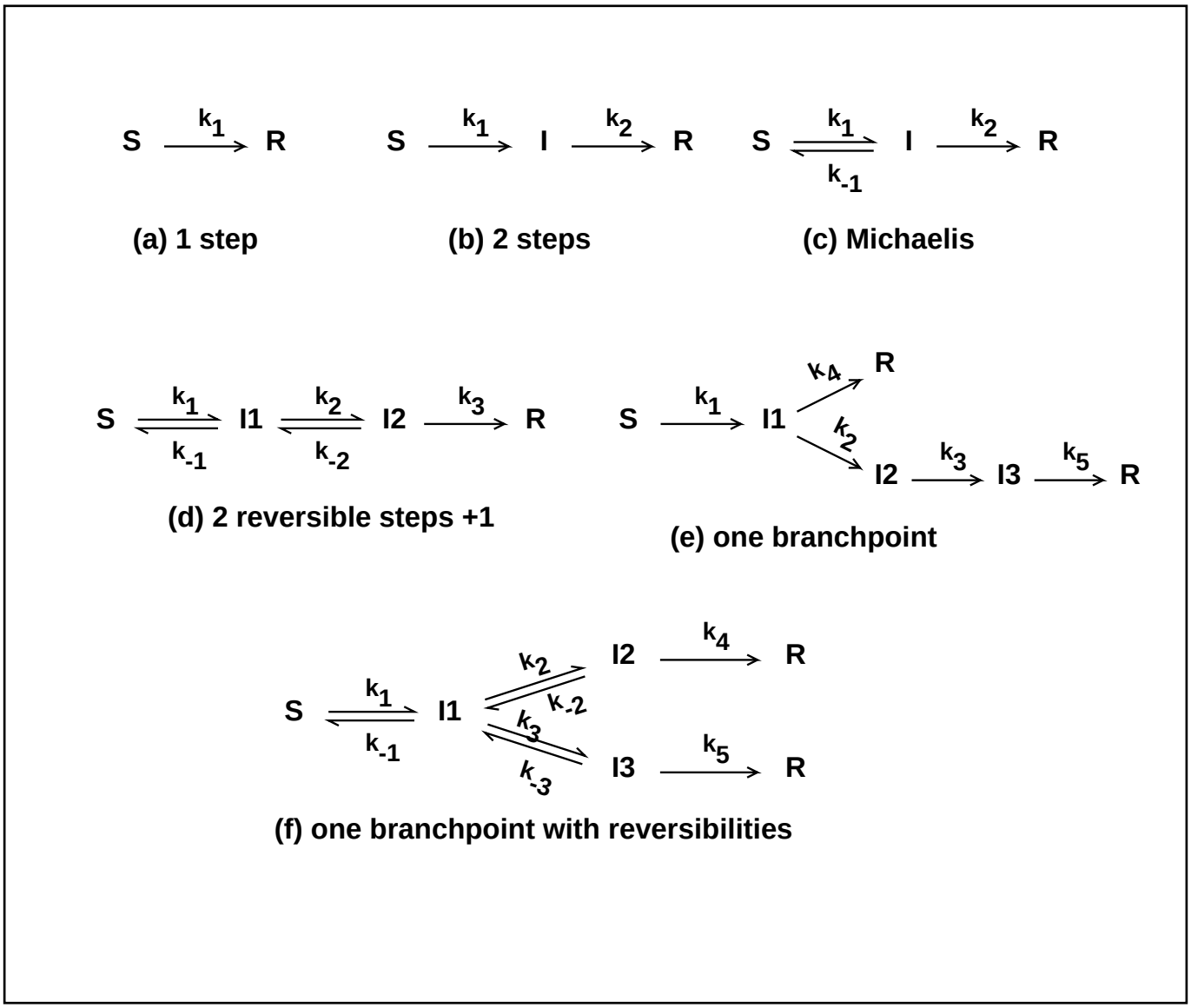
S
k1
R
(a) 1 step
S
k1
I
k2
R
(b) 2 steps
S
k1
k-1
I
k2
R
(c) Michaelis
S
k1
k-1
I1
k2
k-2
I2
k3
R
(d) 2 reversible steps +1
S
k1
I1
k4
R
k2
I2
k3
I3
k5
R
(e) one branchpoint
S
k1
k-1
I1
k2
k-2
k3
k-3
I2
k4
R
I3
k5
R
(f) one branchpoint with reversibilities

**Figure 1**

## Images to compare side by side:

## find the difference protocol

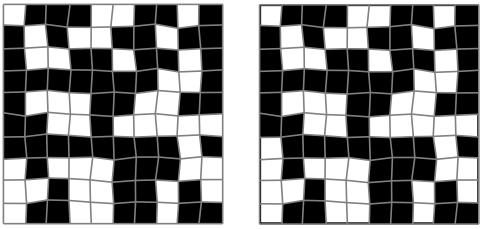

10x10, with grid

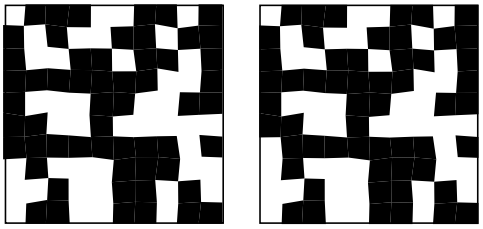

10x10, without grid

## same or different? protocol

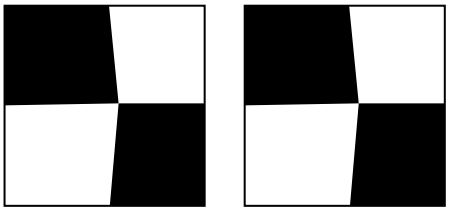

2x2, same

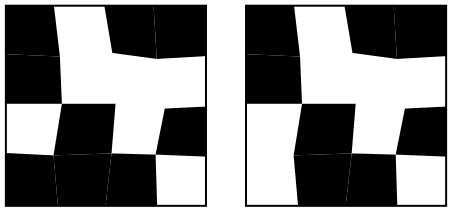

4x4, different

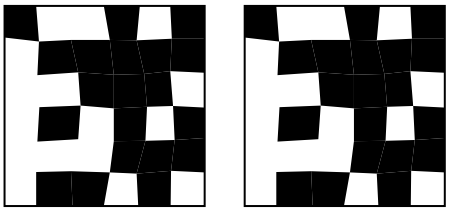

6x6, same

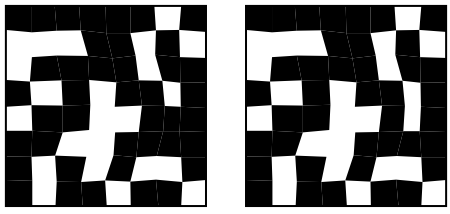

8x8, different

**Figure 2**

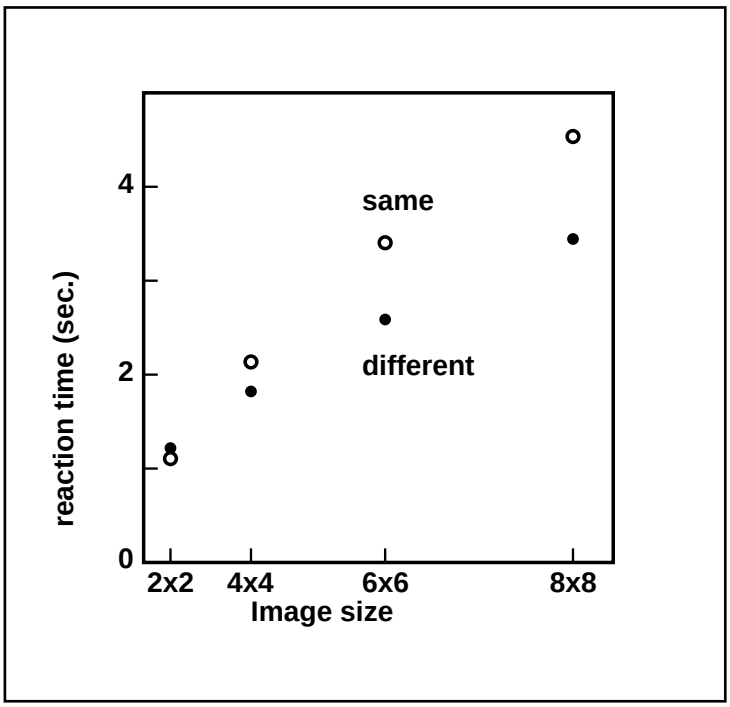
reaction time (sec.)
4
2
0
same
different
2x2
4x4
6x6
8x8
Image size

**Figure 3**

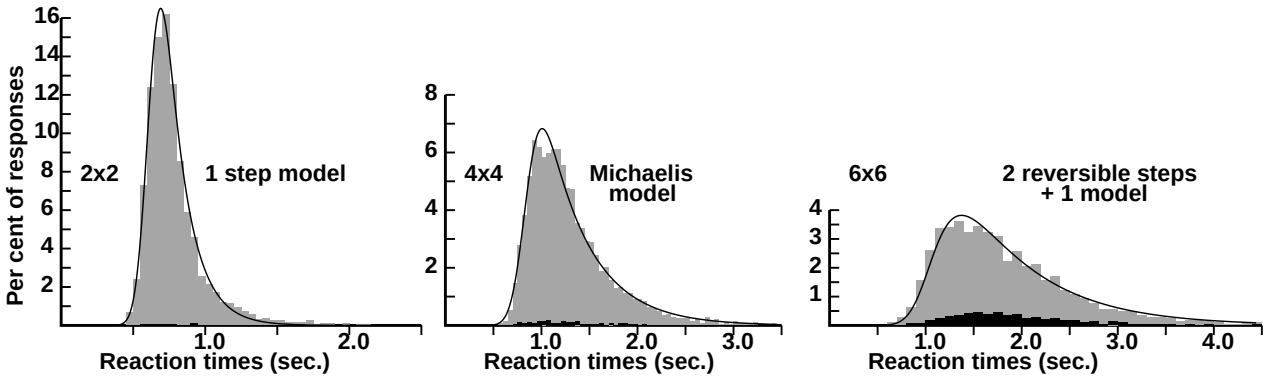


SIDE BY SIDE DIFFERENT IMAGES

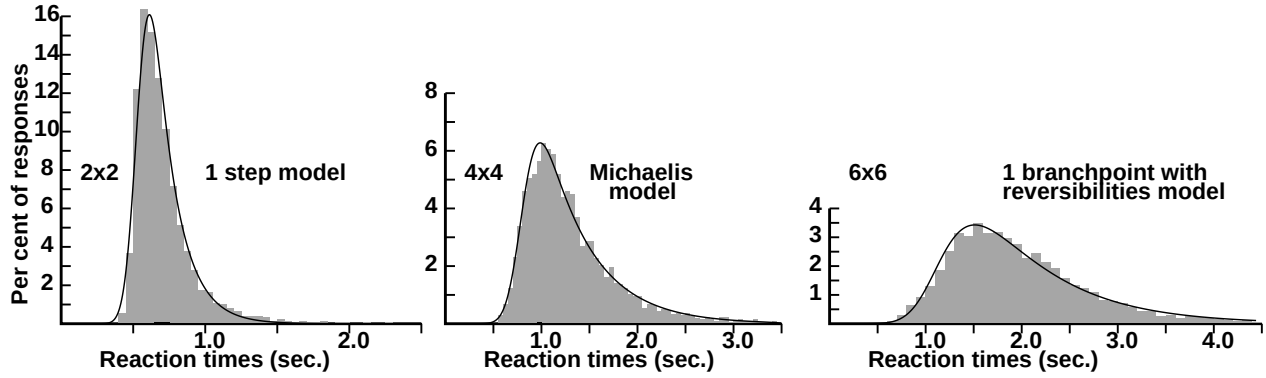


SIDE BY SIDE SIMILAR IMAGES

**Figure 4**

## Symmetry, and symmetry violations

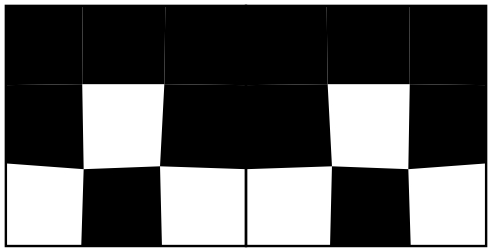

3x3, symmetry

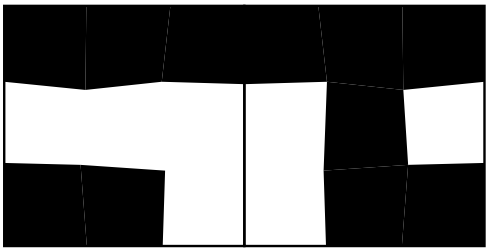

3x3, symmetry violation

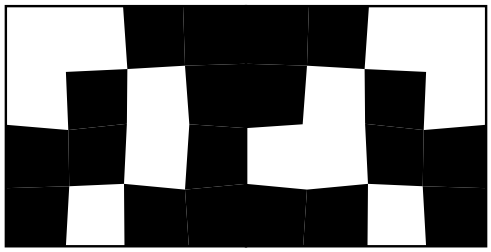

4x4, symmetry violation

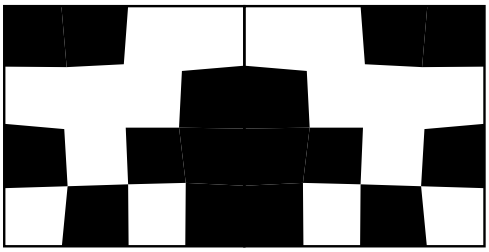

4x4, symmetry

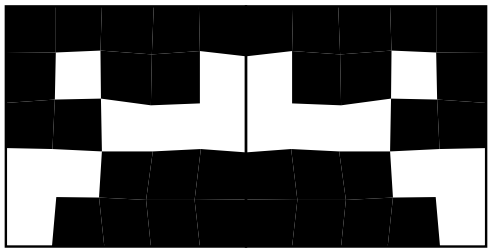

5x5, symmetry

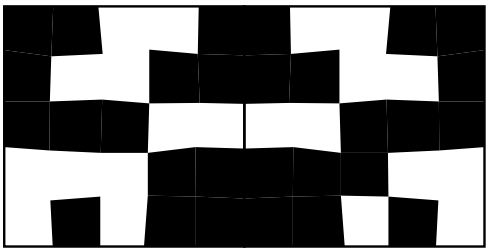

5x5, symmetry violation

**Figure 5**

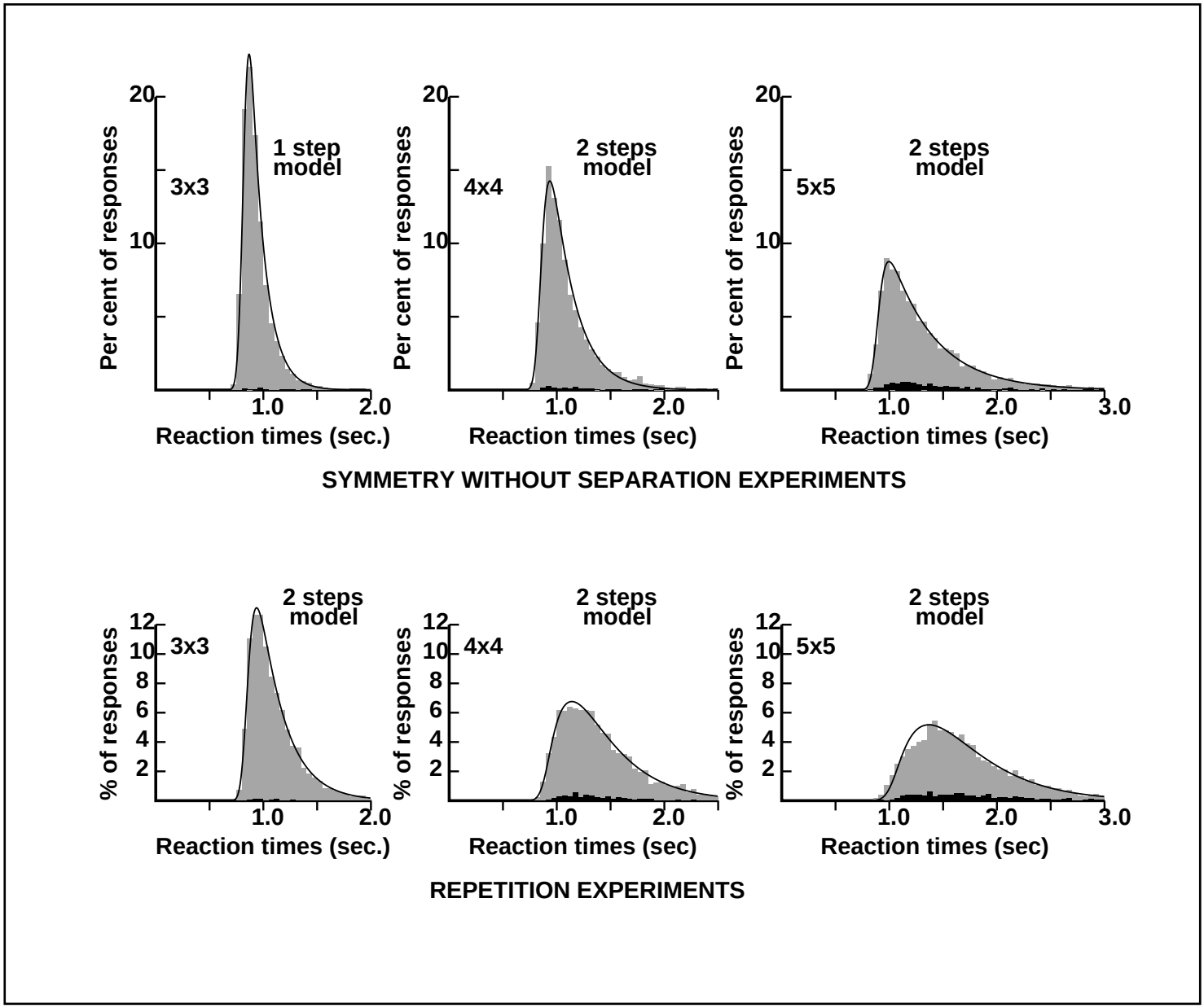
20
10
Per cent of responses
3x3
1 step
model
1.0
2.0
Reaction times (sec.)
4x4
2 steps
model
Reaction times (sec)
5x5
3.0
SYMMETRY WITHOUT SEPARATION EXPERIMENTS
12
8
6
4
2
% of responses
REPETITION EXPERIMENTS

**Figure 6**

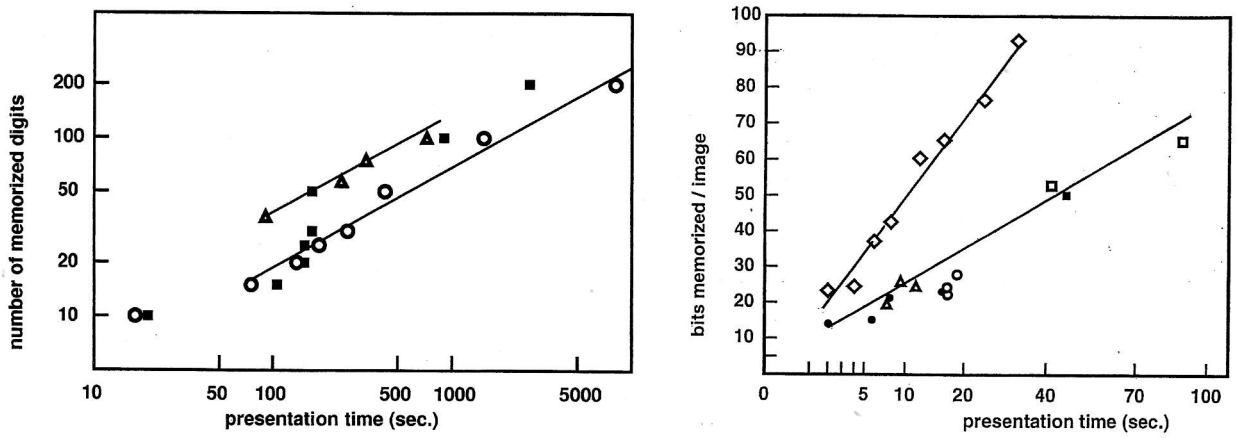
number of memorized digits
200
100
50
20
10
10
50
100
500
1000
5000
presentation time (sec.)
bits memorized / image
100
90
80
70
60
50
40
30
20
10
0
5
10
20
40
70
100
presentation time (sec.)

**Figure 7**

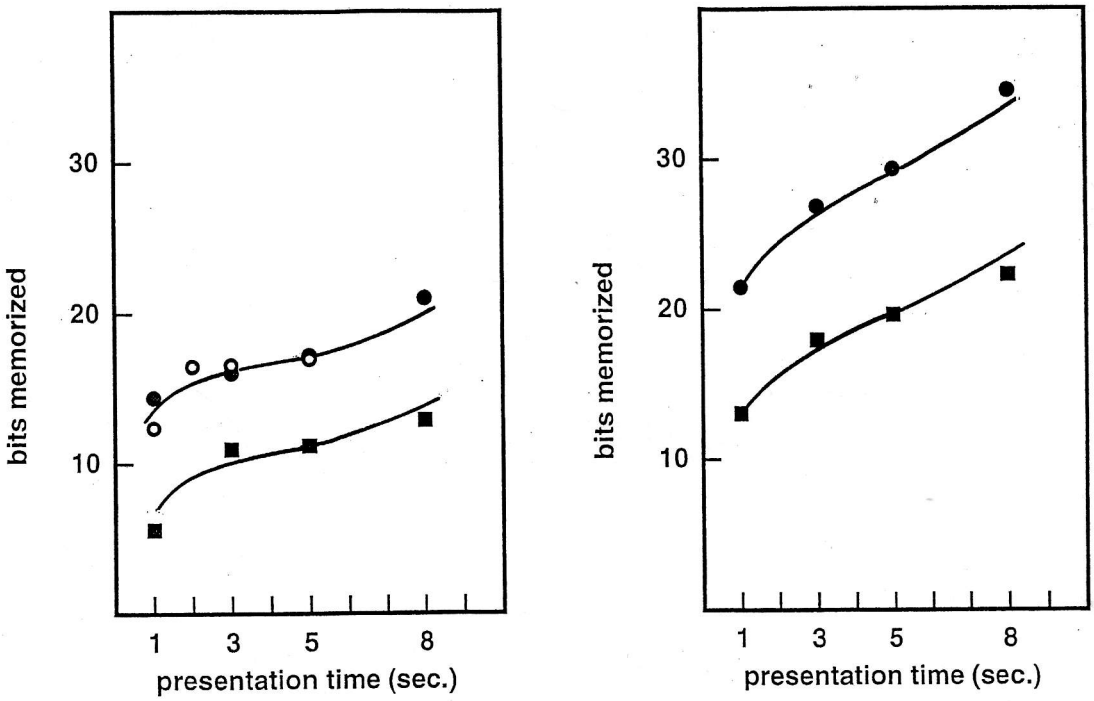
bits memorized
30
20
10
1
3
5
8
presentation time (sec.)
bits memorized
30
20
10
1
3
5
8
presentation time (sec.)

**Figure 8**

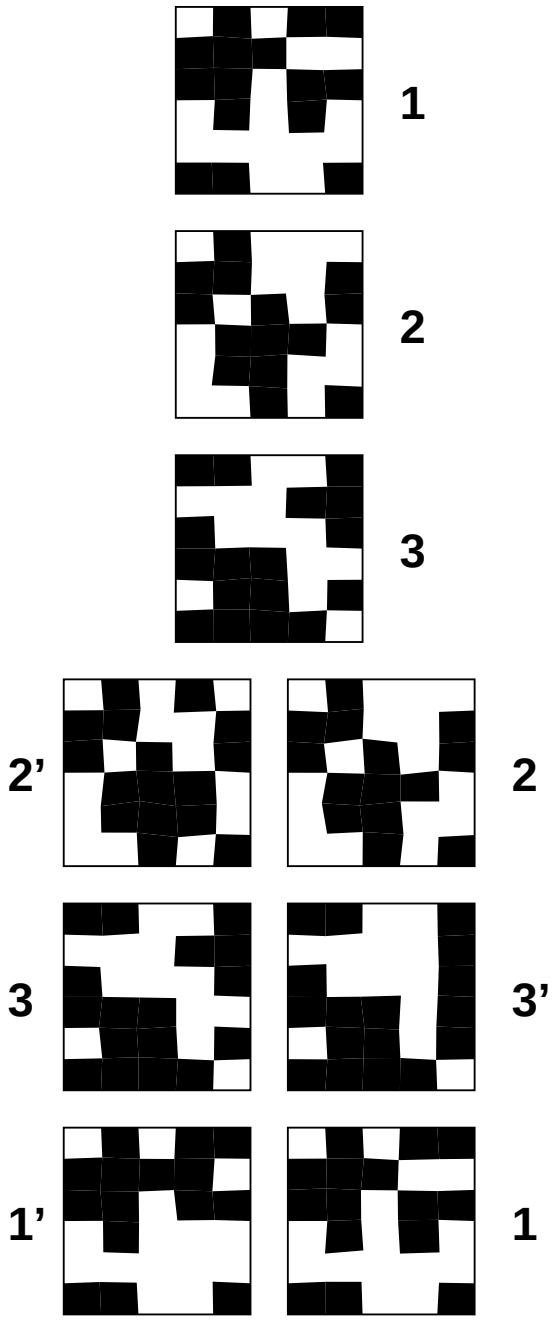


**Figure 9**

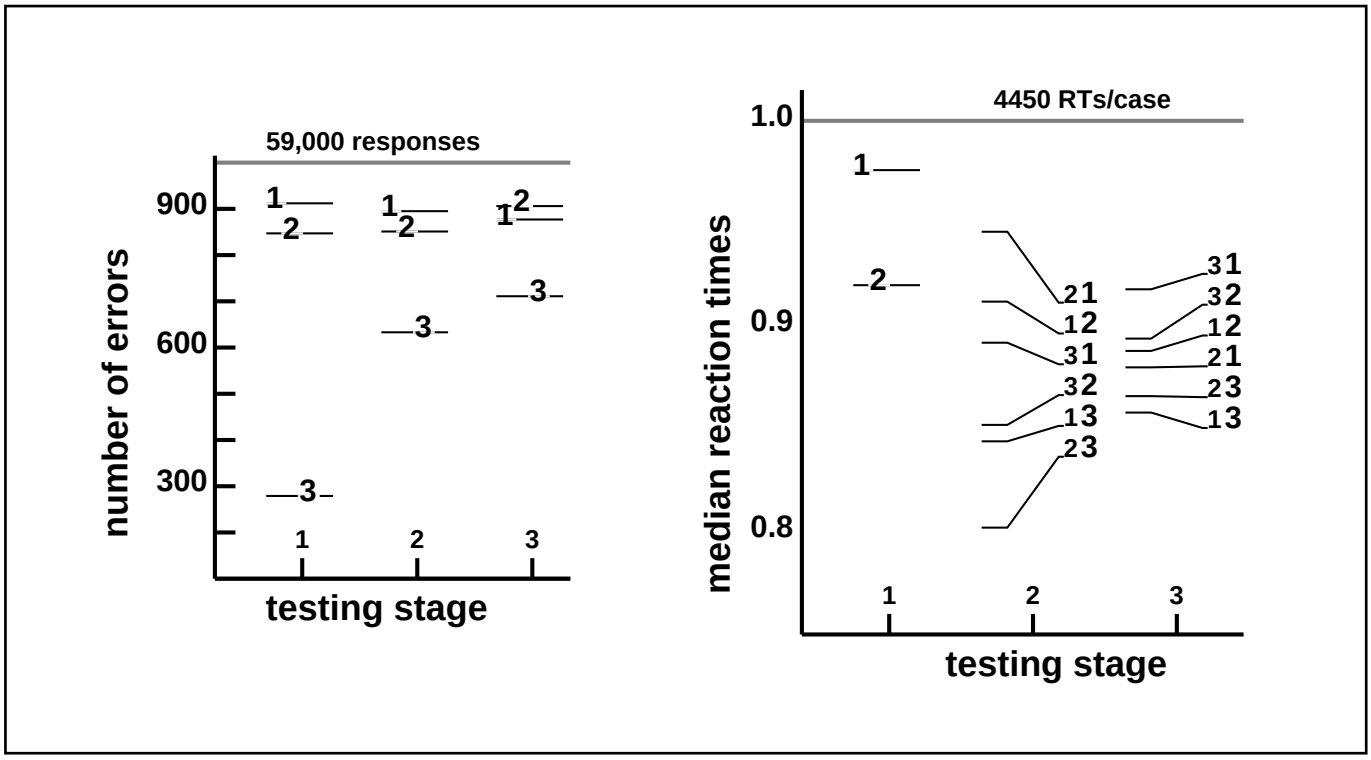
59,000 responses
number of errors
900
600
300
1
2
3
testing stage
4450 RTs/case
median reaction times
1.0
0.9
0.8
21
12
31
32
13
23
testing stage

**Figure 10**

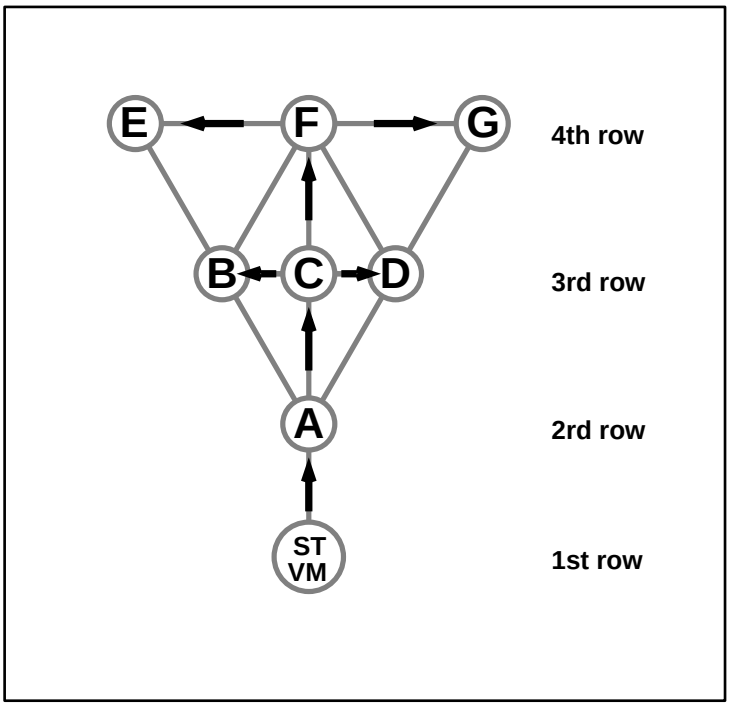


**Figure 11**

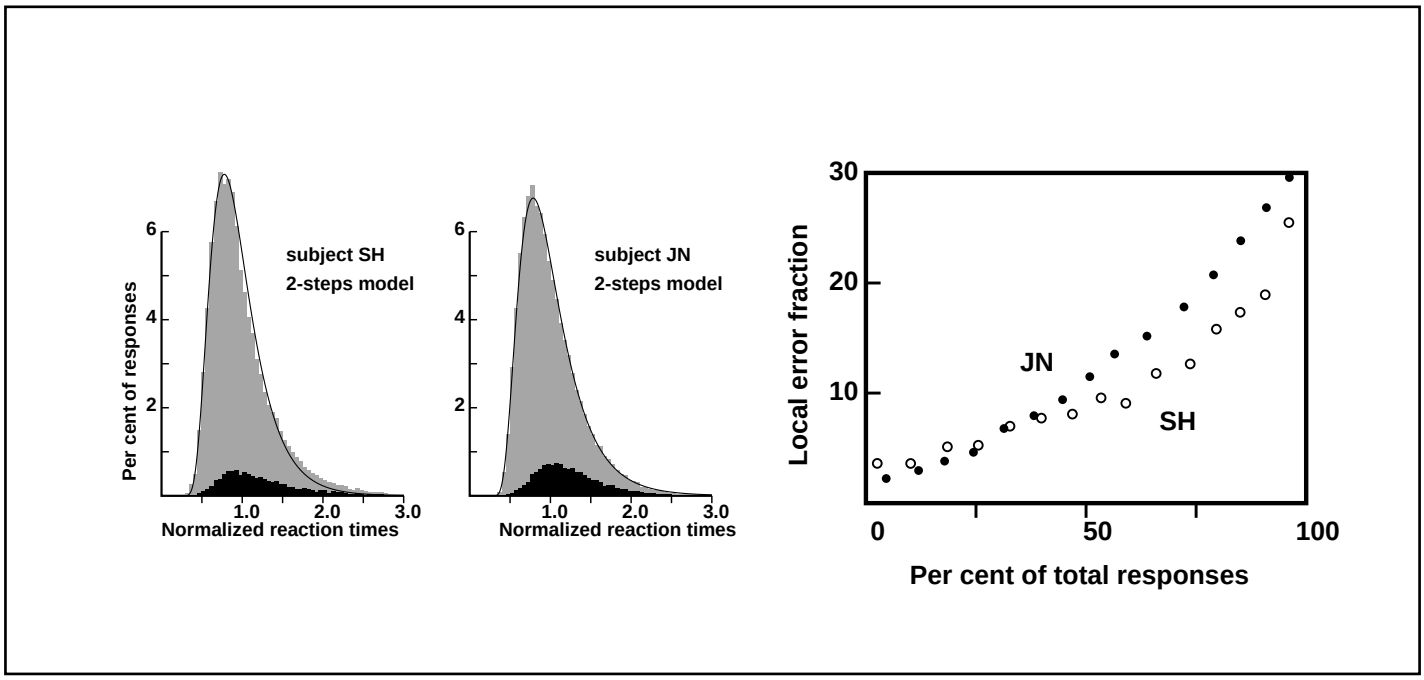
Per cent of responses
6
4
2
subject SH
2-steps model
1.0
2.0
3.0
Normalized reaction times
6
4
2
subject JN
2-steps model
1.0
2.0
3.0
Normalized reaction times
Local error fraction
30
20
10
JN
SH
0
50
100
Per cent of total responses

**Figure 12**

**Image to memorise**

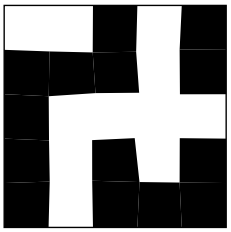

**RECOGNITION TEST:**

**Distractor**

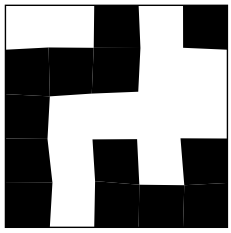

**Test image**

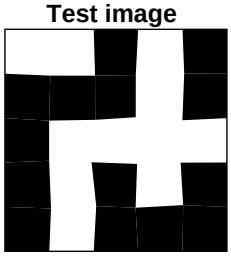

**OR:**

**Test image with inverted contrast polarity**

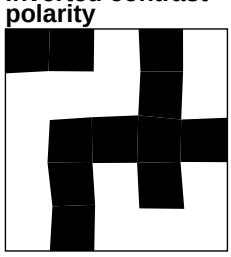

**Distractor**

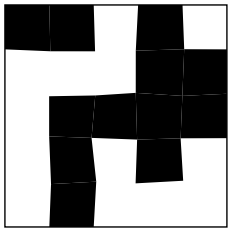

**Figure 13**

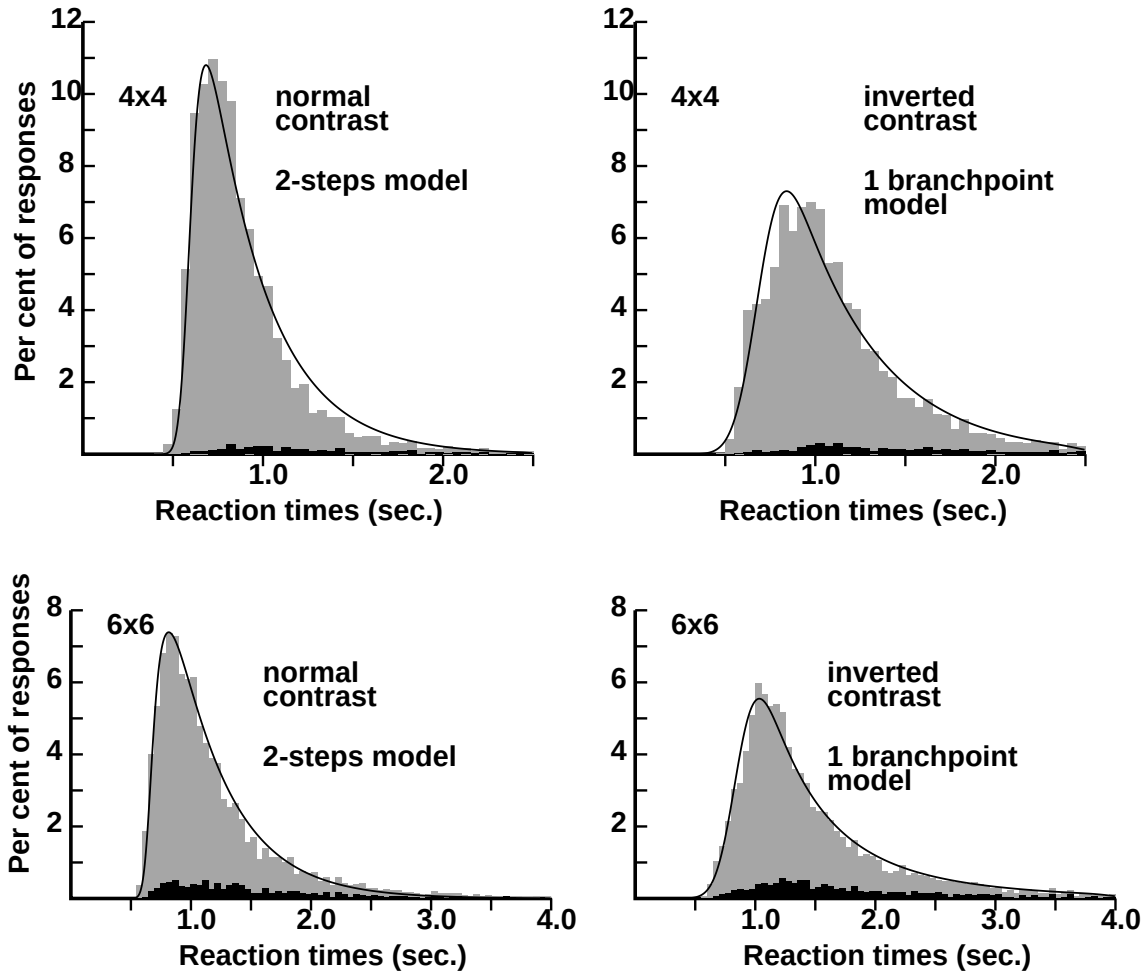
Per cent of responses
12
10
8
6
4
2
4x4
normal
contrast
2-steps model
1.0
2.0
Reaction times (sec.)
4x4
inverted
contrast
1 branchpoint
model
1.0
2.0
Reaction times (sec.)
Per cent of responses
8
6
4
2
6x6
normal
contrast
2-steps model
1.0
2.0
3.0
4.0
Reaction times (sec.)
6x6
inverted
contrast
1 branchpoint
model
1.0
2.0
3.0
4.0
Reaction times (sec.)

**Figure 14**

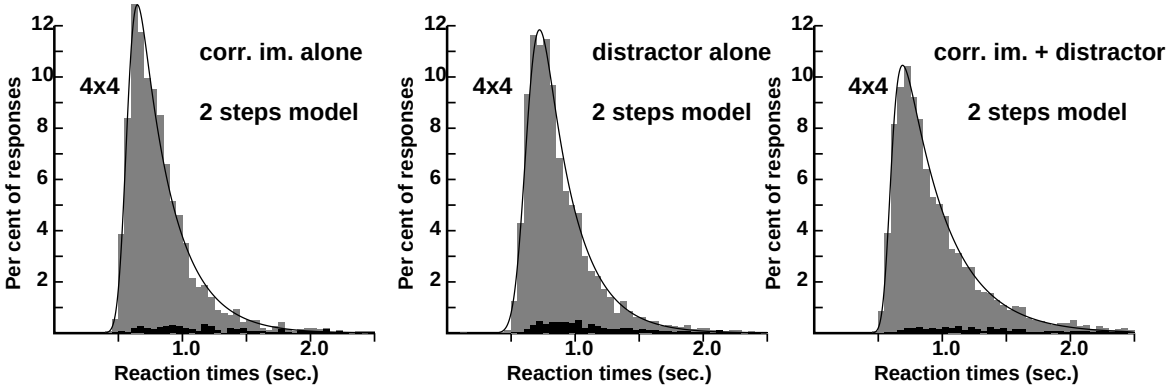
Per cent of responses
12
10
8
6
4
2
4x4
corr. im. alone
2 steps model
1.0
2.0
Reaction times (sec.)
distractor alone
corr. im. + distractor

**Figure 15**

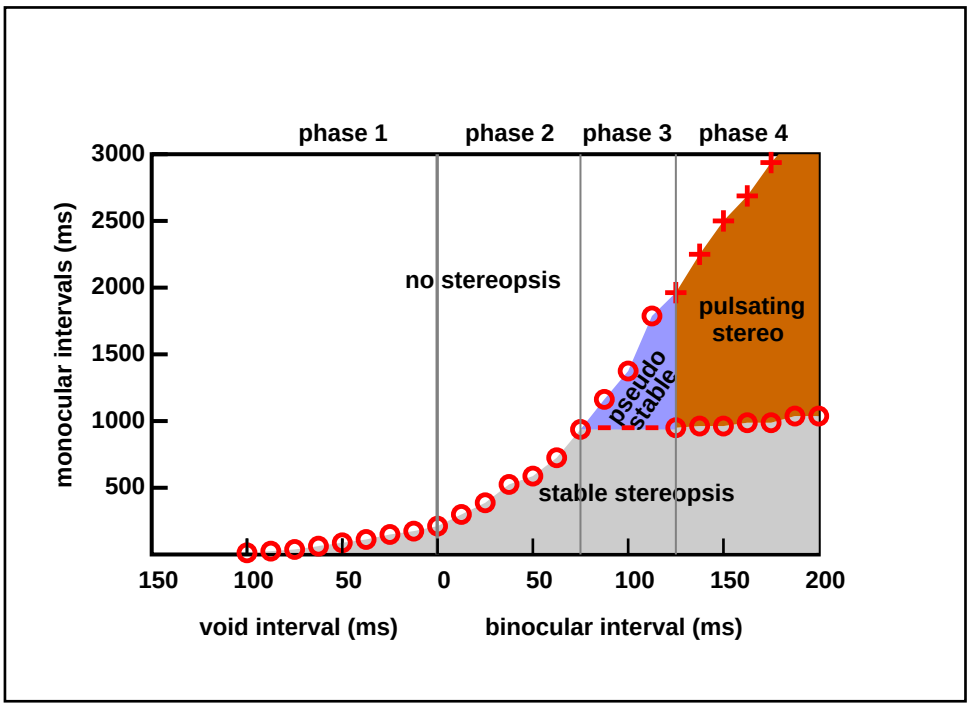
phase 1
phase 2
phase 3
phase 4
3000
2500
2000
1500
1000
500
monocular intervals (ms)
no stereopsis
pulsating
stereo
pseudo
stable
stable stereopsis
150
100
50
0
50
100
150
200
void interval (ms)
binocular interval (ms)

**Figure 16**